Research Report

Towards Understanding COVID-19: Molecular Insights, Co-infections, Associated Disorders, and Aging

Elena L. Paley*
Expert BioMed, Inc. and Nonprofit Public Charity Stop Alzheimers Corp., Miami-Dade, FL, USA

Abstract.

Background: COVID-19 can be related to any diseases caused by microbial infection(s) because 1) co-infection with COVID-19-related virus and other microorganism(s) and 2) because metabolites produced by microorganisms such as bacteria, fungi, and protozoan can be involved in necrotizing pneumonia and other necrotizing medical conditions observed in COVID-19.

Objective: By way of illustration, the microbial metabolite of aromatic amino acid tryptophan, a biogenic amine tryptamine inducing neurodegeneration in cell and animal models, also induces necrosis.

Methods: This report includes analysis of COVID-19 positivity by zip codes in Florida and relation of the positivity to population density, possible effect of ecological and social factors on spread of COVID-19, autopsy analysis of COVID-19 cases from around the world, serum metabolomics analysis, and evaluation of autoantigenome related to COVID-19.

Results: In the present estimations, COVID-19 positivity percent per zip code population varied in Florida from 4.65% to 44.3% (February 2021 data). COVID-19 analysis is partially included in my book *Microbial Metabolism and Disease* (2021). The autoantigenome related to COVID-19 is characterized by alterations in protein biosynthesis proteins including aminoacyl-tRNA synthetases. Protein biosynthesis alteration is a feature of Alzheimer's disease. Serum metabolomics of COVID-19 positive patients show alteration in shikimate pathway metabolism, which is associated with the presence of Alzheimer's disease-associated human gut bacteria.

Conclusion: Such alterations in microbial metabolism and protein biosynthesis can lead to toxicity and neurodegeneration as described earlier in my book *Protein Biosynthesis Interference in Disease* (2020).

Keywords: Aminoacyl-tRNA synthetases, biogenic amines, co-infections, COVID-19, microbial metabolism, necrotizing factor, protein biosynthesis, shikimate pathway, tryptamine, tryptophan metabolism

INTRODUCTION

Alzheimer's disease (AD) and COVID-19 patients have a number of associated diseases including diabetes [1, 2]. Furthermore, pneumonia is a frequent cause of death in both AD and COVID-19 patients [1, 2].

My first intent was to figure out how many COVID-19 positive individuals live in the particular zip code where I live in Miami-Dade, Florida. However, I found no publicly available data on COVID-19 positivity per zip code population density for Florida. Therefore, I collected Internet data on land areas, population, and COVID-19 positivity per zip code, made my own calculations and analysis, and provide the results in the Table 1. Second, we earlier developed the cell and animal

*Correspondence to: Elena L. Paley, Expert BioMed, Inc. and Nonprofit Public Charity Stop Alzheimers Corp., Miami-Dade, FL 33032, USA. E-mail: elena_paley@bellsouth.net.

Table 1
Coronavirus (COVID-19) related positivity in Miami-Dade County and some other Florida Counties (by zip codes) in the period January 29-February 4, 2021. Case data are from Florida's COVID-19 Data and Surveillance Dashboard. Florida Department of Health, Division of Disease Control and Health Protection (https://experience.arcgis.com/experience/96dd742462124fa0b38ddedb9b25e429). Current population is estimated household population for July 2020-February 2021. The estimate is derived from known delivery information, household occupancy rates, household size, and more; based on US Postal Service delivery information (https://www.zip-codes.com). Important: these data do not include population counts for persons in nursing homes, correctional facilities, or other institutions

Zip code	City	Current Population	Land area sq. miles	Number of positive	% Positive per zip code population	Population Density[a]
33154	Surfside, Bal Harbor, Indian Creek	19,883	1.765	1522	7.65	11,265
33143	Kendal	35,771	7.896	4829	13.5	4,530
33031	Homestead	6,603	21.35	649	9.83	309.27
33032	Homestead	61,320	18.828	6758	11.02	3,262
33156	Pinecrest, Kendall	36,242	13.579	3931	10.85	2,669
33033	Homestead	68,700	16.832	7557	11	4,082
32254	Jacksonville, Duval	15,943	12.402	1074	6.74	1,286
33034	Homestead, Florida City	20,442	279.747	2568	12.56	73
33035	Homestead	16,695	20.778	1589	9.51	803.8
32303	Tallahassee, Leon	50,400	35.517	3783	7.51	1,420
32304	Tallahassee, Leon	33,643	15.664	5768	17.14	2,156
33157	Cutler Bay	70,114	14.812	8373	11.94	4,734
34142	Immokalee, Collier	31,734	589.251	3227	10.17	53.87
33139	Miami Beach Lincoln Road	43,540	2.695	5061	11.6	16,155
32607	Gainesville, Alachua	30,518	11.839	2487	8.1	2,586
33140	Miami Beach, flooding zone	27,603	3.051	3059	11.08	9,050
33141	Miami Beach, North Bay Village	42,448	2.323	3752	8.84	18,455
33179	North Miami Beach, Miami Gardens	45,800	5.075	4715	10.29	9,034
33125	Little Havana	54,241	3.905	10351	19.08	13,854
32806	Orlando, Orange	26,754	6.651	1781	6.66	4,504
33142	Liberty City	55,393	7.077	8130	14.68	7,916
33012	Hialeah	72,029	5.859	11417	15.85	12,291
33015	Hialeah	66,159	5.841	9427	14.25	11,328
33178	Francis S. Taylor nature preserve	66,670	56.334	12936	19.4	1,184
33194	Francis S. Taylor wildlife nature preserve	5,662	88.815	1522	26.88	63.76
33605	Tampa, Hillsborough	19,452	7.824	1340	6.88	2,494
33458	Jupiter, Palm Beach	56,115	21.616	3478	6.2	2,598
33401	West Palm Beach, Palm Beach County	32,308	5.202	2945	9.16	6,213
33009	Hallandale, Broward	50,413	5.094	3591	7.1	9,885
33180	Aventura	40,327	3.403	3704	9.18	11,861
33909	Cape Coral, Lee	37,135	17.997	2337	6.29	2,074
34104	Naples, Collier	30,944	9.952	1909	6.17	3,110
34972	Okeechobee	18,439	909.861	1815	9.84	20.26
33496	Boca Raton, Palm Beach	25,685	9.308	1425	5.55	2,762
33498	Boca Raton	15,646	7.426	847	5.41	2,114
33149	Key Biscayne	17,639	4.709	1962	11.1	3,745
33139	Fisher Island	43,593	2.695	5162	11.84	16,175
33136	Overtown, Bayside Marketplace, Jackson Memorial Hospital	16,500	1.427	4132	25.04	11,562
33010	Hialeah	44,499	4.316	7244	16.28	10,324
33134	Coral Gables	40,230	5.216	4234	10.52	7,712
33132	Seybold, Downtown	19,435	1.742	2758	14.2	11,156
33126	Miami	47,985	5.021	7833	16.32	9,559
33130	Downtown, Little Havana	38,950	1.103	5224	13.41	35,409
33128	East Little Havana	8,105	0.397	3597	44.38	20,415
33131	Downtown	28,658	0.407	3059	10.67	63,041
33129	Downtown	16,273	1.351	1640	10.08	12,045
33135	West Flagler	36,278	2.156	4975	13.71	16,826
33139	Miami Beach	43,593	2.695	5171	11.86	16,175
33166	Miami Springs, Doral	26,201	9.548	4358	16.63	2,744
33178	Doral	66,670	56.334	12899	19.35	1,184
33182	Doral, Tamiami	14,321	15.404	2216	15.47	929.9
33122	Miami International Airport	1,152	5.937	452	39.23	194.26

(Continued)

Table 1
(Continued)

Zip code	City	Current Population	Land area sq. miles	Number of positive	% Positive per zip code population	Population Density[a]
33165	University Park	56,017	7.629	9393	16.77	7,342
33054	Opa-locka	30,089	8.769	3672	12.2	3,419
33056	Carol City	37,280	6.079	4227	11.3	6,131
33020	Hollywood, Broward	43,340	6.052	3922	9.05	7,163
33160	Sunny Isles Beach, Golden Beach	62,000	4.246	4433	7.15	14,588
33180	North Miami Beach	40,327	3.403	3754	9.3	11,860
33314	Davie, Broward	28,371	8.373	2844	10.2	3,378
33328	Cooper City, Broward	28,240	9.4	2362	8,36	3,004
33330	Cooper City, Broward	14,896	10.263	1223	8.2	1,446
33029	Pembroke Pines, Broward	47,803	17.348	4427	9.26	2,755
33025	Miramar, Broward	76,495	10.61	7605	9.94	7,216
33024	Hollywood, Broward	73,296	10.727	7784	10.6	6,850
33173	Sunset	34,028	5.07	4188	12.3	6,711
33183	Kendal Lakes	37,620	5.77	5178	13.76	6,520
33193	Kendal West	50,256	7.534	6754	13.4	6,674
33040	Key West, Monroe	35,702	18.5	2714	7.6	1930
33037	Key Largo, Monroe	16,696	33.8	778	4.659	493.6
33323	Sunrise, Broward	24,554	5.994	2028	8.26	4.099
33317	Plantation, Broward	37,455	9.598	3246	8.66	3.901
34236	Sarasota, Manatee	16,284	3.527	758	4.65	4,626
34234	North Sarasota, Manatee	21,254	6.64	1825	8.58	3,200
32967	Winter Beach, Indian River	28,779	41.6	1682	5.84	692
33127	Miami-Dade	29,296	3.302	3165	10.8	8,877
33137	Miami-Dade	30,203	2.023	3659	12.1	14,951
33138	Miami-Dade	29,968	4.218	2381	7.94	7,118
33147	Miami-Dade	49,199	7.255	6101	12.4	6,786
33150	Miami-Dade	30,027	3.494	2704	9.005	8,593
33161	Miami-Dade	52,899	5.467	4661	8.81	9,676
22162	Miami-Dade	46,069	5.191	4346	9.43	8,874
33167	Miami-Dade	19,706	4.143	2044	10.37	4,760
33168	Miami-Dade	25,566	3.683	2378	9.3	6,947
33030	Miami-Dade	36,153	18.371	4927	13.6	1,968

[a]Density of population per sq. miles of the land area. The estimations from July, 2020 to January 2021 based on the Census 2010 population present in the previous publication by Paley [2]. Zip-Codes.com is a non-exclusive licensee (the holder of a license) of the US Postal Service. Miami-Dade County and some other Counties of Florida presented.

models of AD-like neurodegeneration induced by cytotoxic biogenic amine tryptamine produced by human microbiome [3, 4], whereas COVID-19 is known as an aging disease [5]. Thereby my intent was to look for a possible link between our model of neurodegeneration and COVID-19 manifestations. Third, using targeted polymerase chain reaction (PCR) analysis, we demonstrated earlier that AD is associated with specific changes in bacterial profile of human gut microbiome [6]. These changes are associated with alterations in metabolomics [7, 8]. Forth, we immunostained plaques in AD brain with our monoclonal antibodies to human autoantigen tryptophanyl-tRNA synthetase (TrpRS), an enzyme of protein biosynthesis [9, 10]. Moreover, TrpRS is altered in tryptamine-treated cells [11, 12] and induced by interferons [13, 14], whereas tryptamine is an inhibitor of TrpRS and protein biosynthesis.

Fifth, both AD and COVID-19 patients have a number of associated diseases including diabetes [1, 2]. A recent review discusses the potential involvement of microbes residing in the gut and in other body sites in the pathogenesis of eight neuropsychiatric disorders [15].

Sixth, pneumonia is a frequent cause of death in both AD and COVID-19 patients [1, 2]. In this report, the author hypothesizes that deadly pneumonia in both diseases could be a severe necrotizing pneumonia. The hypothetical necrotizing factor might be a cytotoxic tryptamine, a biogenic amine that is able to induce cell death via necrosis and apoptosis at the concentrations that have been found in foods [16] and in some bacteria of human gut [17, 18].

In addition, occurrence of hyperammonemia was reported in COVID-19 patients [19] and in patients with AD [20], while ammonia (NH_3) and hydrogen

peroxide (H$_2$O$_2$) are the products of monoamine amine oxidase (MAO) enzymatic degradation of biogenic amines that present in food and produced by human microbiome. The byproducts of MAO-mediated reactions include several chemical species with neurotoxic potential, such as H$_2$O$_2$, NH$_3$, and aldehydes [21]. Intestinal bacteria produce NH$_3$. The largest amounts of NH$_3$ were generated by gram-negative anaerobes, clostridia, enterobacteria, and *Bacillus spp* [22].

Thus, it is worth analyzing the COVID-19 features derived from: autopsy examination of patients with COVID-19, data on disorders associated with COVID-19, co-infections, metabolomics, and autoantigenome in COVID-19.

The present study is intended to bring attention to different features that may be occurring at the same time as COVID-19 infections. If we know the cause of the COVID-19 related problems, we might be able to figure out how to prevent it happening again.

MATERIALS AND METHODS

COVID-19 data positivity in Florida

Case data are from Florida's COVID-19 Data and Surveillance Dashboard of Florida Department of Health, Division of Disease Control and Health Protection (https://experience.arcgis.com/experience/96dd742462124fa0b38ddedb9b25e429). Current population is estimated household population for July 2020-February 2021. The estimate is derived from known delivery information, household occupancy rates, household size, and more; based on US Postal Service delivery information (https://www.zip-codes.com). Importantly, these data do not include population counts for persons in nursing homes, correctional facilities, or other institutions.

The website Zip-Codes.com includes both the data on population and land area of zip codes. The data included in Table 1 of this article are from at least two Government sources: the Florida Department of Health, Division of Disease Control and Health Protection and the US Postal Service. The estimations from July 2020 to January 2021 are based on the Census 2010 population.

Portions of the data is provided by the US Postal Service from 2021. Zip-Codes.com is a non-exclusive licensee (the holder of a license) of the US Postal Service, a licensed distributor of the US Postal Service ZIP code data (https://www.zip-codes.com/zip-code-database-technical.asp and https://www.zip-codes.com/zip-code-database-testimonials.asp).

There are US Government Organizations among the customers of Zip-Codes.com (https://www.zip-codes.com/zip-code-database-testimonials.asp): Social Security Administration, US Army, US Department of Energy, US Marines, US Navy; Universities: Colorado State University, Columbia University, Cornell University, Dartmouth University, Emory University, Harvard Medical School, MIT, Ohio State University, Stanford University, SUNY University, UC Berkeley, UMass Boston; and other organizations listed by Zip-Codes.com (Datasheer, L.L.C., NY).

Quantification and statistical analysis (Table 2)

Statistical analysis and machine learning

The data included in the Table 2 and in part of the Table 3 were statistically analyzed as described [23]. Specifically, metabolites and therapeutic compounds with over 80% missing ratios in a particular patient group were removed for the metabolomics dataset containing endogenous metabolites while full proteomics features were used for the subsequent statistical analysis. Missing values were imputed with the minimal value and zero in metabolomics and proteomics dataset respectively. Log2 fold-change (log2 FC) was calculated on the mean of the same patient group for each pair of comparing groups. Two-sided unpaired Welch's *t* test was performed for each pair of comparing groups and adjusted *p* values were calculated using Benjamini & Hochberg correction. The statistical significantly changed proteins or metabolites were selected using the criteria of adjust *p* value less than 0.05 indicated and absolute log2 FC larger than 0.25. From the training cohort, authors selected important protein and metabolite features with mean decrease accuracy larger than 3 using random forest. In the random forest analysis, a thousand trees were built using R package randomForest (version 4.6.14) with 10-fold cross validation, and this was repeated for 100 times. The normalized additive predicting probability was computed as the final predicting probability. The larger probability for the binary classification was adopted as the predictive label. For validation in the test cohort 2 (C3) generated by targeted proteomics and metabolomics, z-score normalization was applied before running the model validation. Those selected important features were used for the random forest analysis on the independent test cohort. The authors also ran

Table 2

Metabolites related to shikimate pathway in human sera of severe-COVID-19, non-severe COVID-19 and non-COVID-19 patients in comparison with healthy individuals and severe versus non-severe COVID-19 (fold change, FC, statistically significant). The data on metabolites are from the article by Shen et al., 2020 [23]

Metabolites	Severe-COVID-19 versus healthy FC	Non-COVID-19 versus healthy FC	Non-severe COVID-19 versus healthy FC	Severe/nonsevere COVID-19 FC
Benzoate	6.31	6.245	6.31	
5-Hydroxyindoleacetate			−1.1246	
Genistein sulfate[a]			−1.896	
Hippurate	−1.466		−1.034	
Histidine			−0.5148	
Indoleacetate			−0.39	
Methyl–4-hydroxybenzoate sulfate			−4.483	
N-Acetyltryptophan	−0.5		−0.492	
Quinate (quinic acid)	−0.49	−0.973	−2.49	
Serotonin	−1.725	−0.542	−1.046	
Tryptophan	−0.567		−0.6395	
Tryptophan betaine	−3.3		−2.696	
Tyramine O-sulfate	−3.446		−3.213	
Tyrosine			−0.32	
Kynurenate	1.1868	3.726		1.37
Kynurenine	1.23	1.295		1.197
Quinolinate (quinolinic acid)[b]	1.64	2.9		1.488
Phenylalanine		0.397		
Indolepropionate	−1.00158	−2.82		

[a]Genistein is monoamine oxidase (MAO) inhibitor [118]. [b]Increased proinflammatory cytokine levels have been shown to activate the kynurenine pathway, which causes increased production of quinolinic acid (QA, an N-Methyl-D-aspartate agonist) and decreases in the synthesis of serotonin. QA exerts many deleterious effects on the brain via mechanisms including N-methyl-D-aspartate excitotoxicity, increased oxidative stress, astrocyte degeneration, and neuronal apoptosis [119].

the randomForest analysis with omics features after z-score normalization and got same classification results [23].

Statistical tests, p values

In the reported studies discussed here, a significant test result means $p < 0.05$ [24].

RESULTS AND DISCUSSION

Analysis of COVID-19 positivity percentage by zip code's population in Florida, USA

The characteristics such as percentage of COVID-19 positivity per population of zip codes and dependence of COVID-19 positivity on population density by zip codes in Florida are not publicly available. Thus, the Florida residents, visitors, and public are not aware of the percentage of COVID-19 positive residents living in particular neighborhood. Meanwhile, knowledge of percentage of COVID-19 virus positivity per zip code population could give a clue in understanding the virus origin and dispersion and thus may help to prevent the virus dispersion.

For February 4, 2021: Total FL Residents Tested: 188,595, FL Residents Positive: 10,946, FL

Residents Negative: 177,649; Percent Positive: 5.80%; Total cases: 1,731,931; Total Population: 20,598,139; Positive: 8.408%. Cumulative Data for Florida Residents: Positive Residents: 1,739,276. Cumulative data for resident hospitalizations: 74,267 or 0.36% per total Florida population; cumulative Florida resident deaths: 27,599 (data posted on February 6, 2021) (https://experience.arcgis.com/experien ce/96dd742462124fa0b38ddedb9b25e429). Of note, the percentage of Florida population in 2018 over the age of 65 was 20.5% (https://www.prb.org/ which-us-states-are-the-oldest/). California state's total population that was age 65 or older in 2018 was only 14.3%. In contrast, 20.6% of Maine's population was age 65 or older, the highest share of any state, followed closely by Florida with 20.5%. Although COVID-19 is considered as age-related disease, the percentage of hospitalized COVID-related Florida residents is much less (0.36%) than the percentage of aging population ≥ 65 (20.5%). Up to 80% of those dying of COVID are in long-term care, translating to the possibility that over a third of mortality are those afflicted with AD, since approximately half of those in long-term care have AD [5]. The comorbidities of aD further align with COVID's risk factors: diabetes, heart disease, and minority status. Importantly,

Table 3
Levels and effects of benzoate and its metabolite hippurate in human diseases and medical conditions

N	Medical Conditions/Diseases	Benzoate	Hippurate	References
1	COVID-19 severe/healthy	↑ 6.3-fold, sera		[23]
	COVID-19 severe/healthy		↓ –1.4667-fold, sera	[23]
2	COVID-19 non-severe/healthy	↑ 6.3-fold, sera		[23]
3	COVID-19 non-severe/healthy		↓ –1.0344-fold, sera	[23]
4	COVID-19 non-severe/healthy		↓ 4-hydroxyhippurate –1.1247-fold, sera	[23]
5	Non-COVID-19/healthy[a]	↑ 6.245-fold, sera		[23]
6	Alzheimer's disease		↑ 3.8-fold, plasma	[121]
7	Mild cognitive impairment	↑ 2.0-fold PABA, CSF	↑ 4.55-fold, plasma	[121]
8	Fetal growth restriction	↑ 3.1-fold, urine		[122]
9	Challenges in children with severe atopic dermatitis	100 mg/reactions, 3/6		[123]
10	Overweight subjects	Benzoate → anthranilic acid ortho-aminobenzoic acid, blood		[124]
11	Crohn's disease		↓ 2.73, urine	[125, 126]
12	Crohn's disease	5 mg/ml benzoate → hippurate, urine	↑ ~4.6-fold, percentage change, 1h post-dose, urine	[126]
13	Colorectal cancer	↓ 1.71 para-aminobenzoate PABA, feces	↑ 1.24-fold, % prevalence, feces	[127]
14	Bacterial vaginosis		↓ 0.08-fold, cervicovaginal lavage fluid	[128]
15	Cigarette smoking		↓ 4-fold, vaginal	[129]
16	Urea cycle disorders, acute episodes of hyperammonemia, infection	Intravenous median 250 mg/kg, over 2 h ammonium decrease		[130]
17	Fatigue		↑ plasma	[131]

[a]Non-COVID-19 patients had overlapping symptoms with COVID-19 patients, such as fever, cough, headache, fatigue, expectoration, chest tightness and some common comorbidity including hypertension, respiratory system and digestive system [23].

respiratory issues are common among most late-stage AD patients [5]. Patient Auguste described by Alzheimer had four vascular disorders: diabetes mellitus, decubitus angina, arteriosclerosis, and stupor, which altogether caused widespread atrophy of her brain resulting in severe dementia with pronounced language disorders [25].

Even more intriguingly, recent reports show that newly diagnosed diabetes is commonly observed in COVID-19 patients [26].

Some states, including Colorado, Illinois, Maryland, Nevada, New Jersey, and South Carolina, regularly release cumulative data on cases and deaths at specific facilities. California, Massachusetts, Michigan, and Ohio, among others, provide some details on the number of cases—but not on deaths. Others report aggregate totals for their state but provide no information on where the infections or deaths have occurred [27]. Wang et al. retrospectively evaluated all patients with a confirmed diagnosis of bacterial infection at a tertiary general hospital in Jining, China for the period between January 2012 and December 2014 [28]. Bacterial identification and susceptibility testing were performed. The authors screened a total of 15,588 patients, out of which

7,579 (48.6%) had a hospital-acquired infections (HAIs) [28]. HAIs, also called nosocomial infections, affect the clinical outcomes in hospitalized patients and represent a serious concern worldwide [29]. Tsalik et al. reported in 2016 [29] that infection poses a substantial risk to hospitalized patients, particularly those in intensive care units (ICUs). Recent estimates indicate that 1.7 million HAIs occur annually in US hospitals, costing $9.8 billion and causing approximately 100,000 deaths. Hospital-acquired pneumonia, including ventilator-associated pneumonia, accounts for approximately 20% of all HAIs; however, the high mortality rate of 10 to 50% results in the greatest relative number of HAI deaths (~36,000 annually) [29]. The base-case analysis assumed 17.6% of ventilated patients and 11.2% of nonventilated patients develop hospital-acquired infection and that 28.7% of patients with hospital-acquired infection experience delays in appropriate antibiotic therapy with standard care [29].

Case data used here for analysis of percentage of COVID-19 positivity and corresponding population density by zip codes are from Florida's COVID-19 Data and Surveillance Dashboard, Florida Department of Health, Division of Disease Control and

Health Protection. Data are updated daily. Comparison of counties is not possible because case data are not adjusted by population. Therefore, here COVID-positivity data are adjusted by population. The percentage of COVID-positivity and current population density are presented in Table 1 for 82 zip codes of Florida. The lowest percent of COVID-19 positivity was seen in Boca Raton, known as one of the wealthiest cities in South Florida with 5.4% positivity, in Jupiter with 6.2% positivity of population, the home of Scripps Research Institute (https://www.scripps.edu/campuses/florida/), and in Key Largo with 4.659%. Key Largo of Monroe County is the island in the upper Florida Keys. The ∼3-fold higher percent (14.68%) of population was estimated for Liberty City (zip code 33142) of Miami-Dade County. Increasing numbers of lower-income elderly and welfare-dependent families migrated to Liberty City after their displacement primarily from inner city Overtown, turning the area into a dangerous, low-income ghetto (https://en.wikipedia.org/wiki/Liberty_City_(Miami)). In Overtown, 25% of population was COVID-positive. In Surfside, there was 7.65% COVID-19 positivity and population density of 11,265, while in Kendal, a 13.5% COVID-positivity and population density of 4,530 were estimated. Both cities were located in Miami-Dade County, FL. This exemplify that COVID-19 positivity is not directly correlated with the population density. The cities located in the north part of Florida, including Gainesville, Tallahassee, Jacksonville, Orlando, and Tampa, had a low positivity from 6.6 to 8.1%. The highest percent, 44.38%, was estimated for a population of 8,105 in zip code 33128 that includes East Little Havana, the Cuban neighborhood in Miami Dade, FL. East Little Havana is a neighborhood where high crime rates and gang activity is still a concern. The distance between Miami International Airport (MIA) and Little Havana is 3 miles. A 39.23% positivity was estimated in the small population of MIA (zip code 33122). Little Havana located just west of downtown Miami. Little Havana (zip code 33125) showed 19.08% COVID-positivity. Zip codes 33194 with 26.88% and 33178 with 19.4% positivity include residential areas in close proximity to Francis S. Taylor wildlife nature preserve.

Therefore, one can suggest that some factor/s other than COVID-positive humans might be a source of the virus spread. Moreover, in a comparative analysis (Table 1), a high percentage of COVID-19 positivity (44.3% at west of downtown Miami, 25% in Overtown, 19% in Little Havana,

19.35% in Doral, and 16.28% in Hialeah) may indicate that ecological and social factors affecting COVID-19 positivity of particular populations should be taken into the account. Positivity percentage in cities located at north of Florida with 6.6 to 8.1%, at west (Naples, Collier-6.17%, Sarasota, Manatee-4.65%, and Cape Coral-6.29%), at east (Surfside-7.65%, Sunny Isles Beach, Golden Beach-7.1%), and at south of Florida (Key Largo with 4.659%) may indicate that COVID-related virus did not travel from North, West, East, and South borders to reach inland areas with a highest positivity up to 44.38% in zip code 22128. Key Biscayne and Fisher Island with 11.1% and 11.84% COVID-positivity, respectively, locate close to the neighborhood with a high positivity. The distance between East Little Havana and Fisher Island, the richest zip code in the US, is 7 miles via MacArthur Causeway. Distance between zip code 33136 including Overtown and zip code 33128 including East Little Havana is 1.1 mile.

Thus, East Little Havana is at the epicenter of COVID-19 concern in Florida.

Miami-Dade administration informs that eligible residents (18+, No Symptoms Required) living in target zip codes may call to request a COVID-19 test (PCR Test At-Home Testing) to be performed at their home: North Miami, Little Haiti, Upper East Side, Little River, Liberty City, Little Havana, Allapattah, Homestead/Florida City. Eligible zip codes include 33127, 33137, 33138, 33147, 33150, 33161, 33162, 33167, 33168, 33125, 33128, 33130, 33135, 33142, 33030, 33033, and 33034 (https://www.miamidade.gov/global/initiatives/coronavirus/covid19-location.page?Mduid_covid19-location=cov1606766547000993). Of this list of target zip codes, zip codes 33125 and 22128 that include Little Havana show highest positivity percent in my estimations (Table 1). All the Miami Dade Government target zip codes are included in the Table 1.

After the nearly 800 families in what Bloomberg calls the richest ZIP code in America became concerned about COVID-19, they did not wait in long lines for a test.

Fisher Island has its own health clinic, operated by the University of Miami Health System. The wealthy community is paying for newly available antibody testing for all of its residents—half of whom are older than 60—and its staff, from housekeepers to marina workers. Some 1,250 employees and residents have been tested thus far, according to a spokeswoman for the community (https://www.cnn.com/2020/04/16/

us/fisher-island-miami-coronavirus-antibody-testing /index.html). Zip code 33139 that includes Fisher Island showed 11.84% of COVID-19 positivity (Table 1). Fisher Island is about seven minutes by boat from Miami Beach and 7 miles from Little Havana via MacArthur Causeway.

Both AD and COVID-19 are age-dependent diseases with a high prevalence of obesity and diabetes [1, 23]. Moreover, the recent meta-analysis of eight studies with more than 3,700 patients shows a pooled proportion of 14.4% for newly diagnosed diabetes in hospitalized COVID-19 patients [26].

The cumulative data until February 6, 2021 show that 0.36% of the total Florida population was hospitalized with a diagnosis of COVID-19.

1.722% (5.7 million people in the US population of 331 million people) have been diagnosed with AD. Thus, the rate of AD is 4.79-fold higher than the rate of COVID-19-positive disease. Median time from AD dementia diagnosis to death was 3.8 years [30]. Therefore, the prevalence of COVID-19 severe disease in Florida, USA is essentially lower than prevalence of another age-dependent disease AD that considered by National Institute on Aging to be non-infectious.

On August 3, 2020, total positive cases in Florida were 491,884; negative 3,260,914; death 7,157. Positive cases by exposure source on August 3, 2020 indicated as traveled 3,737; contact with confirmed case 133,732; travel & contact with confirmed case 3,756; under investigation 323,681; Total 491,884. Thus, the source/s for majority of positivity was not known.

Possible sources of COVID-19 virus

The recent CDC data indicate the virus linked to COVID-19 has been found in untreated wastewater (https://www.cdc.gov/coronavirus/2019-nc ov/community/sanitation-wastewater-workers.html). The leakage of untreated wastewater happened previously during some storms, hurricanes, and consequent flooding in Miami, Florida and New York City, NY.

Fecal microorganisms including viruses can be dispersed due to the sewage spills. Particularly, Fort Lauderdale, Florida leaked 232 million gallons of sewage from its failing pipes over a three-month period earlier in 2020. In addition, accidental rupturing of three sewer lines in Miami Beach, Florida between July 2019 and March 2020 dumped about

1.7 million gallons of wastewater into Biscayne Bay (reported by Martin Vassolo, The Miami Herald, November 10, 2020). A spokesperson for the Department of Environmental Protection (DEP) could not answer questions about how often the agency sues municipalities for sewer spills because enforcement statistics were not readily accessible.

The medical procedure of fecal microbiota transplantation (FMT) can also spread microorganisms causing diseases. FMT, also known as a stool transplant, is the process of transferring fecal bacteria and other microbes from one organism into the gastrointestinal tract of another. Changes observed in the recipient's biology are routinely attributed to bacterial cells in the donor feces ($\sim 10^{11}$ per gram of human wet stool). Bojanova and Bordenstein (2016) [31] examined the literature and summarized findings on the composition of fecal matter in order to raise cautiously the profile of its multipart nature. In addition to viable bacteria, which may make up a small fraction of total fecal matter, other components in unprocessed human feces include colonocytes ($\sim 10^7$ per gram of wet stool), archaea ($\sim 10^8$ per gram of wet stool), viruses ($\sim 10^8$ per gram of wet stool), fungi ($\sim 10^6$ per gram of wet stool), protists, and metabolites [31]. Despite the promising results of FMT in treatment of recurrent *Clostridium difficile* infections, several barriers remain, including determining the characteristics of a healthy microbiome [32]. Since the first modern descriptions of its use in 1958 [33], FMT has increasingly gained interest and rapid acceptance during the last 10 years [34]. However some infections acquired during FMT become life-threatening [35]. In three healthy volunteers, FMT caused long-term (~ 1 year of observation) changes of the gut microbiota with the shift toward donor microbiota composition. One of three volunteers developed a systemic inflammatory response syndrome after FMT [36].

The Food and Drug Administration (FDA) published on March 1, 2016 the Enforcement Policy Regarding Investigational New Drug Requirements for Use of Fecal Microbiota for Transplantation to Treat Clostridium difficile Infection Not Responsive to Standard Therapies (https://www.federalregister. gov/documents/2016/03/01/2016-04372/enforceme nt-policy-regarding-investigational-new-drug-requir ements-for-use-of-fecal-microbiota-for; Document Citation: 81 FR 10632, Agency/Docket Number: Docket No. FDA-2013-D-0811, Document Number: 2016-04372).

Lawrence J. Brandt, MD, Professor of Medicine and Surgery of Albert Einstein College of Medicine,

Bronx, New York reported in 2012 [37] that worldwide, approximately 450 cases of fecal transplantation for treatment of *C. difficile* have been reported. Dr. Brandt performed his first fecal transplantation in 1999 [37].

It was reported in 2019 that fecal microbiota transplantation is a promising way to treat colorectal cancer [38]. In *EBioMedicine*, Li and colleagues showed that FMT with feces of patients with colorectal cancer accelerating the progression of adenoma to adenocarcinoma could cause chronic inflammation and disturb the ecological balance of the mice's gut microbiota [39]. The gavage of fecal samples from patients with colorectal cancer promoted the intestinal carcinogenesis in both germ-free and control conventional mice [40].

Infectious diseases commonly spread through the direct transfer of bacteria, viruses, or other germs from one person to another. Thereby, despite the promising results, FMT procedure can have negative effects on human health through spreading untested, unknown, and uncultivable microorganisms related to illnesses of unknown etiology. Fecal tests that were positive for SARS-CoV-2 were reported in 8 studies [41, 42]. Severe acute respiratory syndrome coronavirus 2 (SARS-CoV-2) causes coronavirus disease 2019 (COVID-19) [42].

Chang et al. found recently large variation in predicted reopening risks based on mobility network models of COVID-19: on average across metro areas, full-service restaurants, gyms, hotels, cafes, religious organizations, and limited-service restaurants produced the largest predicted increases in infections when reopened. Reopening full-service restaurants was particularly risky [43].

SARS-Cov 2 was present in some air samples that were collected from patients' rooms in hospitals [44].

Pneumonia, necrotizing infections, COVID-19 case reports at autopsy and co-infections

Those dying with, but not of, COVID-19 may still be infectious

Accumulating evidence shows that microbial co-infection increases the risk of disease severity in humans. There have been few studies about SARS-CoV-2 co-infection with other pathogens. In the retrospective study by Zhu et al., 257 laboratory-confirmed COVID-19 patients in Jiangsu Province, China were enrolled from January 22 to February 2, 2020 [45]. They were re-confirmed by real-time RT-PCR and tested for 39 respiratory pathogens. In total, 24 respiratory pathogens were found among the patients, and 242 (94.2%) patients were co-infected with one or more pathogens. Bacterial co-infections were dominant in all COVID-19 patients, *Streptococcus pneumonia* was the most common, followed by *Klebsiella pneumonia* and *Haemophilus influenzae*. Most co-infections occurred within 1–4 days of onset of COVID-19 disease. In addition, the proportion of viral co-infections, fungal co-infections and bacterial-fungal co-infections were the highest in severe COVID-19 cases. There were 10, 22, 20, and 13 pathogens found in symptomatic, mild, moderate, and severe/critical cases, respectively. *S. pneumoniae*, *K. pneumoniae*, *H. influenzae*, fungi Aspergillus, EB virus, *Escherichia coli*, and *Staphylococcus aureus* were simultaneously found in four clinical groups. *Moraxella catarrhalis* and *Acinetobacter baumannii* were found in asymptomatic category, mild category and moderate category [45]. The 81 patients (31.5 %) had viral co-infection, 236 (91.8 %) had bacterial co-infection, and 60 (23.3 %) had fungal co-infection [45].

Lacy et al. (2020) [46] presented a case (Snohomish County Medical Examiner's Office, Everett, WA, USA) of sudden unexpected death due to COVID-19 as a means of illustrating common autopsy findings, as well as diagnostic and biosafety considerations. The authors also review and summarize the current COVID-19 literature in an effort to provide practical evidence-based biosafety guidance for medical examiner-coroner offices encountering COVID-19 at autopsy. While in some cases, a history of fever and/or respiratory distress (e.g., cough or shortness of breath) may suggest the diagnosis, epidemiologic studies indicate that the majority of individuals infected with COVID-19 develop mild to no symptoms. Those dying with—but not of—COVID-19 may still be infectious, however [46]. Swabs of the right and left main bronchi were procured. The reverse transcriptase–polymerase chain reaction (RT-PCR) results for SARS-CoV-2 returned as positive 11.5 hours after submission. Negative influenza results returned several days later. Bacterial cultures were positive for methicillin-sensitive *Staphylococcus aureus* and *Streptococcus viridans*. The lack of acute histologic inflammation in the lungs was observed. Based on the autopsy and investigative findings, and in accordance with US National Vital Statistics certification guidelines, the cause of death was determined to be acute respiratory distress syndrome (ARDS) due to viral pneumonia due to COVID-19. Other essential contributory factors

included type 2 diabetes mellitus, hypertension, and obesity. In this case [46], the lungs were moderately heavy and edematous (right: 818 g, left: 705 g). Hilar and mediastinal lymph nodes appeared enlarged. The heart exhibited moderate coronary atherosclerosis in each of the main coronary distributions, but there were no occlusions or critical stenoses. The myocardium was free of obvious infarcts. There was moderate infrarenal aortic atherosclerosis. The kidneys were finely granular and had focal cortical scars. The brain exhibited hydrocephalus ex vacuo.

Therefore, the co-infections with *Staphylococcus aureus* and *Streptococcus viridans* are not defined as a cause of death or contributory factors in this case [46]. The authors interpret that "given the lack of acute histologic inflammation in the lungs, the bacterial culture results were interpreted as being most likely contaminants or postmortem artifact" [46]. However, the review by Bauer et al. (2006) reveal that ARDS is frequently associated with bacterial infections [47]. Moreover, the Japanese case of 34-year-old woman with ARDS due to methicillin-resistant *Staphylococcus aureus* sepsis in hyper-IgE syndrome was reported by Sato and colleagues [48].

Hereby death cause of COVID-19 virus-positive cases is uncertain. Thus, the statistics of certification defining the cause of death due to COVID-19 is a contentious issue. In other words, COVID-19 death can be due to different causes of related or unrelated underlying diseases and conditions. Correlation of corona virus positivity and death in a low percentage of population might have even just been noise. Of course, correlation is not causation; the shift toward death with corona virus positivity could have been due to any number of other issues, such as co-infections, and/or other overt, covert and inadvertent conditions.

Goursaud et al. reported COVID-19 necrotizing pneumonia and extracorporeal membrane oxygenation as a challenge for anticoagulation [49]. High levels of anticoagulation must be considered with caution in the most severe patients with SARS-CoV-2 necrotizing pneumonia [49].

COVID-19 and bacterial co-infections: biogenic amines in Staphylococcus aureus, necrotizing pneumonia

Necrotizing pneumonia has been described in COVID-19 fatal case in France [49]. Necrotizing pneumonia is known to be associated with fungal or bacterial co-infection, especially *Staphylococcus aureus*, which is one of the major causes of death

following virus influenza infection [50]. In the genus Staphylococcus, certain species are capable of producing trace biogenic amines through the activity of staphylococcal aromatic amino acid decarboxylase (SadA). SadA decarboxylates aromatic amino acids to produce trace biogenic amines. SadA-expressing staphylococci were prevalent in the gut of most probands, where they are part of the human intestinal microflora. Furthermore, sadA-expressing staphylococci showed increased adherence to human colorectal adenocarcinoma HT-29 cells and 2- to 3-fold increased internalization. Internalization and adherence was also increased in a sadA mutant in the presence of tryptamine [17, 18]. Of note, tryptamine can induce necrosis [16]. Therefore, tryptamine and other trace biogenic amines can play a role in necrotizing pneumonia.

Bacterial meningitis is an inflammation of the meninges which covers and protects the brain and the spinal cord. Such inflammation is mostly caused by blood-borne bacteria that cross the blood-brain barrier (BBB) and finally invade the brain parenchyma. Pathogens such as *Streptococcus pneumoniae*, *Neisseria meningitidis*, and *Haemophilus influenzae* are the main etiological causes of bacterial meningitis. Furthermore, clinical studies have shown indications of meningitis-caused dementia [51].

Twelve different biogenic amines formation in 58 isolates of *Streptococcus thermophilus* from home-made natural yogurt were investigated in histidine (HDB) and lysine decarboxylase broth (LDB). Tryptamine produced at mg/L concentrations in both HDB and LDB [52]. In HDB, tryptamine was produced at 1–100 mg/L in 47 *S. thermophilus* isolates while in LDB, 7 isolates produced 101–500 mg/L tryptamine [52]. HDB and LDB contained 1 g peptone, 0.5 g Lab-Lemco powder, 2.5 mg NaCl, 4.01 g L-histidine monohydrochloride monohydrate or L-lysine monohydrochloride, and 2.5 mg pyridoxal HCl in 500 mL distilled water; the pH was adjusted to 5.5 with 1 M KOH or 6% trichloroacetic acid.

These data suggest that *S. thermophilus* strains can use histidine and lysine decarboxylases for production of tryptamine, phenylethylamine, tyramine, serotonin, and dopamine or HDB and LDB that included peptone and Lab-Lemco powder contained sufficient amount of tryptophan (16 mg/L), to be decarboxylated by tryptophan decarboxylase. The authors concluded that the other biogenic amines are likely to have been produced from the amino acids in peptone and beef extract [52]. Two isolates of *S. thermophilus* produced significant amounts of tyramine,

504 and 539 mg/L while tyrosine was calculated at 14 mg/L. The formation of dopamine by *S. thermophilus* ranged from 1.17 to 2160 mg/L. Tryptamine was not determined in 10 HDB and 14 LDB cultivated *S. thermophiles* isolates.

Therefore, tryptamine unlikely derived from HDB or LDB alone. However, some strains could metabolize tryptamine and other biogenic amines. Thus, the biogenic amines content in HDB and LDB should be estimated and controlled.

Tryptamine was produced by *Klebsiella pneumoniae* in HDB and by *K. pneumoniae* and *Pseudomonas putida* in LDB [53].

Food industries consider *S. thermophilus* as non-pathogenic.

In 2018, tryptamine (0 to 120.18 ± 4.29 mg/kg) and other biogenic amines were reported to be produced by bacterial strains isolated from the popular fermented soybean product from 15 different regions in China [54]. Some of these strains were able to degrade biogenic amines [54].

Of note, in this study published by the journal *Scientific Reports* (Nature Publishing Group) [54], the data on content of biogenic amines in soybean extracts are provided, but no data available on a content of biogenic amines in the media for cultivation of bacterial isolates for the detection of biogenic amines. Meanwhile, LB medium composed of NaCl, 10 g/L Tryptone, 10 g/L, and Yeast Extract, 5 g/L and used for bacteria cultivation may contain biogenic amines that can be degraded by some bacterial strains thus effecting results on biogenic amines analysis.

The seven tryptamine-producing bacteria were isolated in South Korea from commercial salted and fermented sand lance (*Ammodytes personatus*) fish sauces using an L-tryptophan decarboxylating medium. These tryptamine-producing bacteria, identified using an API kit and 16S rRNA analysis, included *Lysinibacillus xylanilyticus* (one strain), *Lysinibacillus fusiformis* (four strains), and *Staphylococcus epidermidis* (two strains). *Lysinibacillus* spp. produced the highest levels of tryptamine in culture broth containing 0.5% L-tryptophan, compared with 1.0% and 2.0% preparations. After 72 h of incubation, *Staphylococcus epidermidis* produced the highest levels of tryptamine (60.50 μg/mL and 664.86 μg/mL) in culture broth containing 2.0% L-tryptophan [55]. Thus, Staphylococcus strains producing high amount of tryptamine can originate from food including Korean fish sauces.

Staphylococcus aureus strain HZW450 isolated (China: Hangzhou, Submitted 11-APR-2017, State Key Laboratory for Diagnosis and Treatment of Infectious Diseases, The First Affiliated Hospital College of Medicine Zhejiang University, China) from pus of a patient with impetigo (highly contagious skin infection) possess pyridoxal-dependent decarboxylase (GenBank: ATH56183.1; 472 amino acids; pyridoxal-deC, DOPA decarboxylase family). High amino acid sequence identity to pyridoxal-deC (3e-157, 99.08%) presents in the nasal sample (anterior nares) of a male participant (emb|ODTW01004449.1; Submitted 01-SEP-2017) from the dbGaP study "HMP Core Microbiome Sampling Protocol (USA control set). Hangzhou, the capital of Zhejiang province in China, was confronted with the pandemic of a novel coronavirus (COVID-19) that originated in Wuhan, Hubei province. According to the Health Commission of Zhejiang Province, the 6 cases were first reported on January 19, 2020, and the cumulative cases reached 169 as of February 20, 2020. The situation in Hangzhou was once rather severe—it was the top-ranking city with respect to the number of confirmed cases in Zhejiang province at the beginning of the epidemic [56]. Therefore, the bacterial *Staphylococcus aureus* strain possessing gene for DOPA decarboxylase was isolated from human sample in China before the first cases of COVID-19 reported. Similar gene presents in the human sample in the US.

McDanel and colleagues reported in 2016 that *Staphylococcus aureus* is a common cause of respiratory infections, including pneumonia, and can lead to necrotizing pneumonia and death. Influenza complicated by *S. aureus* co-infection can progress rapidly to death within a week of symptom onset [57]. Increased mortality rates associated with *Staphylococcus aureus* and influenza co-infection was investigated in Maryland and Iowa in the US [57]. In this study, the researchers retrospectively analyzed data for 195 respiratory infection patients who had positive *Staphyloccocus aureus* cultures and who were hospitalized in two hospitals in Iowa and Maryland during 2003–2009. Odds for death for patients who also had influenza-positive test results were > 4 times higher than for those who had negative influenza test results [57]. This dataset did not include information about variables such as influenza vaccination status, mechanical ventilation, co-infection with organisms other than influenza and *S. aureus*, and whether the pneumonia was necrotizing [57]. The characterization of biogenic amine production by *S. aureus* clinical isolates is not available.

Up to 75% of those infected with influenza that go on to acquire pneumonia, are confirmed to have bacterial co-infection [50].

The mouse model used by Jia et al. (2018) to explore coinfection-induced death [58]. To minimize the impact of the pathogens themselves on coinfection-related mortality, various coinfection sequences and time points were planned using nonlethal doses of influenza virus (PR8) and *S. aureus* (MRSA). The results indicated that mortality is related to the sequence and timing of infection with both pathogens. Specifically, mortality was highest (> 80%) in mice infected with MRSA [d, d-1, d-2, and d-3 groups from day 0 to day 3 post-infection with influenza virus, which was higher than that in other co-infected groups [58].

Despite invasive aspergillosis being reported in immunocompetent severe COVID-19 patients [59, 60], other pathogen profiles are not yet established, and descriptive clinico-microbiological studies are still warranted [49]. Fungi *Aspergillus niger* transformed tryptamine into 5-hydroxyindole-3-acetamide [61].

Sharifipour and colleagues [62] reported (September 2020) the study of nineteen critically ill patients admitted to ICU wards in two referral hospitals for coronavirus in Qom, Iran. These patients were enrolled in the study of bacterial infections in COVID-19 patients [62]. Patients were given antibiotics such as ceftriaxone and azithromycin before admission to the ICUs. Inclusion criteria were being infected by COVID-19, hospitalized, intubated, and mechanically ventilated > 48 h in ICUs [62]. Of nineteen COVID-19 patients, 11 (58%) patients were male and 8 (42%) were female, with a mean age of ~67 years old. The 16 of 19 patients had diabetes. The average ICU length of stay was ~15 days and at the end of the study, 18 cases (95%) expired and only was 1 case (5%) discharged. In total, all patients were found positive for bacterial infections, including seventeen *Acinetobacter baumannii* (90%) and two *Staphylococcus aureus* (10%) strains. There was no difference in the bacteria species detected in any of the sampling points. Seventeen of 17 strains of *Acinetobacter baumannii* were resistant to the evaluated antibiotics [62]. Overall, it is important to limit the risk of infection and the spread of these resistant strains through controlling nosocomial infections accurately and bringing secondary infections caused by resistant bacteria that can increase the mortality rate in COVID-19 critical patients into attention [62].

Taking into account that high proportion of COVID-positive patients had preexisting diabetes (16 of 19 COVID-positive patients had diabetes in Iran [62]), it is worth to look into possibility that diabetic patients could be infected during insulin administration. Grissinger reported in 2017 that "wrong patient" insulin pen injections are alarmingly frequent in the US [63]. The insulin pen sharing could lead to pathogen transmission. The large-scale potential exposures to blood-borne pathogens caused by using insulin pens for multiple patients after changing the needle include: 2,114 patients at a Texas Army medical center in 2009; 2,345 patients at a Wisconsin clinic in 2011; 716 patients at a New York Veterans Affairs medical center in 2013; 1,915 patients at a New York general hospital in 2013; 3,149 patients at a Connecticut hospital in 2014 [63].

During the 1918–1919 pandemic, the bacteria most often recovered from the sputum, lungs, and blood of pneumonia patients, alive or dead, were common colonizers of the upper respiratory tracts of healthy persons, i.e., *Hemophilus influenzae*, *Streptococcus pneumoniae*, *S. pyogenes*, and/or *Staphylococcus aureus* [64]. Brundage and Shanks (2008) hypothesize that infections with the pandemic influenza strain generally caused self-limited (rarely fatal) illnesses that enabled colonizing strains of bacteria to produce highly lethal pneumonias [64]. They suggest opportunities for prevention and treatment during the next pandemic with bacterial vaccines and antimicrobial drugs, particularly if a pandemic strain-specific vaccine is unavailable or inaccessible to isolated, crowded, or medically underserved populations [64].

Morens, Taubenberger, and Fauci of the National Institute of Allergy and Infectious Diseases, National Institutes of Health, Bethesda, MD reported in 2008 that the majority of deaths in the 1918–1919 influenza pandemic likely resulted directly from secondary bacterial pneumonia caused by common upper respiratory–tract bacteria. Less substantial data from the subsequent 1957 and 1968 pandemics are consistent with these findings [65]. In this study of the postmortem samples from people who died of influenza during 1918–1919, the authors revealed the uniformly exhibited severe changes indicative of bacterial pneumonia. Bacteriologic and histopathologic results from published autopsy series clearly and consistently implicated secondary bacterial pneumonia caused by common upper respiratory–tract bacteria in most influenza fatalities [65].

Wunderink and Waterer [66] reported in 2014 that pneumonia is sometimes referred to as the

forgotten killer. The World Health Organization estimates that lower respiratory tract infection is the most common infectious cause of death in the world (the third most common cause overall), with almost 3.5 million deaths yearly. Together, pneumonia and influenza constitute the ninth leading cause of death in the US, resulting in 50,000 estimated deaths in 2010. This number is probably underestimated, since deaths from sepsis (for which pneumonia is the most common source) and deaths attributed to other conditions (e.g., cancer and AD) for which pneumonia is the terminal event are coded separately [66]. Clinical features suggesting community-acquired methicillin-resistant *Staphylococcus aureus* (MRSA) pneumonia are: cavitary infiltrate or necrosis; rapidly increasing pleural effusion; gross hemoptysis (not just blood-streaked); concurrent influenza; neutropenia; erythematous rash; skin pustules; young, previously healthy patient; severe pneumonia during summer months [66]. According to European Centre for Disease Prevention and Control since 31 December 2019 and as of 02 November 2020, 46 597 299 cases of COVID-19 (in accordance with the applied case definitions and testing strategies in the affected countries) have been reported, including 1,201,162 deaths (COVID-19 situation update worldwide, as of November 2, 2020 https://www.ecdc.europa.eu/en/geographical-distribution-2019-ncov-cases).

The first New York case was reported in early March 2020 and by the first week in April, the New York Presbyterian Hospital system, including Columbia and Weill Cornell, had close to 2,500 in-patients with over 700 patients on ventilators [67]. The standard of care for COVID-19 was supportive care only with essential morbidity and mortality recognized. An emerging crisis without proven treatments COVID-19 is a mild illness in more than 80% of people infected, but about 15% will require hospitalization and about 5% intensive care unit support.

Epidemiology, clinical course, and outcomes of critically ill adults with COVID-19 in New York City were reported by Cummings et al. [68] and by Goyal et al. [69]. The authors concluded that critical illness among patients hospitalized with COVID-19 in New York City is common and associated with a high frequency of invasive mechanical ventilation, extrapulmonary organ dysfunction, and substantial in-hospital mortality [68]. The incidence of bacterial superinfection in the setting was unknown early in the outbreak in the study reported by Cummings et al. [68]. In the study by Goyal et al., bacteremia (the

presence of bacteria in the bloodstream) was revealed in 19/338, 4.8% (all), 15 (11.9%) of invasive mechanical ventilation (N = 130); 4 (1.8%) of no invasive mechanical ventilation (N = 263). The viral co-infection was revealed in 4/393, 1.0% (all), 2 (1.5%) in invasive mechanical ventilation and 2 (0.8%) in no invasive mechanical ventilation [69]. In-hospital treatment included hydroxychloroquine, remdesivir, and oral corticosteroids [69]. This report characterizes the first 393 consecutive patients with COVID-19 who were admitted to two hospitals in New York City [69]. Of note, no treatment with antibiotics indicated for the COVID-positive patients. Among these patients, obesity reported for 35.8%, diabetes - 25.2%, hypertension-50.1%, chronic obstructive pulmonary disease (COPD)-5.1%, asthma-12.5%, coronary artery disease-13.7%, death-10.2%. Infiltrates on initial chest radiograph (during hospital stay) were revealed in 75.3% of the COVID-19 patients, and no data provided on the infectious agents in the infiltrates. All these diseases including COPD [70] and asthma [71] was found to be associated with increased risk of dementia [1], whereas nursing home patients have been disproportionately affected by COVID-19. It has been reported that one-fourth of all COVID-19 deaths nationwide occurred in nursing homes and other long-term care facilities [72]. Analyses of Connecticut, New Jersey, and New York indicate that nursing homes with higher percentages of Medicaid patients were more likely to have COVID-19 deaths [72]. Among the 1,162 nursing homes in this study, 184 (15.8%) had 6 or more COVID-19 associated deaths [72].

Therefore based on this study [69] bacteremia and to a lesser extent viral co-infection in COVID-19 patients are related to Invasive Mechanical Ventilation in New York City Hospitals.

Sen-Crowe et al. reported (2020) that in Florida, the overall and July, 2020 case-fatality ratios (CFRs) remain low at 1.4% and 0.90%, respectively [73]. California reports a CFR of 1.8% since the onset of the pandemic and 1.1% in July 2020. The state of Texas reports an CFR of 1.4% overall and in the past month (July 2020) [73].

Postmortem studies of COVID-19 patients all over the world

Pomara, Li Volti, and Cappello published the article in 2020 [74]: COVID-19 Deaths: Are We Sure It Is Pneumonia? Please, Autopsy, Autopsy, Autopsy!

Salerno and collogues from Italy published the review article in 2020 "No Autopsies on COVID-19

Deaths: A Missed Opportunity and the Lockdown of Science" [75]. The authors of this review state that despite the increasing number of published studies on COVID-19, in all the examined studies the lack of a well-defined pathophysiology of death among patients who died following COVID-19 infection is evident. Autopsy should be considered mandatory to define the exact cause of death, thus providing useful clinical and epidemiologic information as well as pathophysiological insights to further provide therapeutic tools. A total of 50 articles met the inclusion criteria. However, only 7 of these studies reported autopsy-based data. The analysis of the main data from the selected studies concerns the complete analysis of 12,954 patients, of whom 2,269 died (with a mortality rate of 17.52%). Laboratory confirmation of COVID-19 infection was obtained in all cases and comorbidities were fully reported in 46 studies. The most common comorbidities were: cardiovascular diseases (hypertension and coronary artery disease), metabolic disorders (diabetes, overweight, or obesity), respiratory disorders (chronic obstructive pulmonary disease), and cancer. The most common reported complications were: ARDS, acute kidney injury, cardiac injury, liver insufficiency, and septic shock. Only 7 papers reported histological investigations. Nevertheless, only two complete autopsies are described, and the cause of death was listed as COVID-19 in only one of them. The lack of postmortem investigation did not allow a definition of the exact cause of death to determine the pathways of this infection. Based on the few histopathological findings reported in the analyzed studies, it seems to be a clear alteration of the coagulation system: frequently prothrombotic activity with consequent thromboembolism was described in COVID-19 patients.

The article published by Sperhake [76] provides an overview of the status of the autopsy series published worldwide and shows the path taken by the city of Hamburg in Germany, where autopsies are ordered by the health authorities in the interests of disease control. The risk of infection posed by SARS-CoV-2-positive deceased persons may be overestimated [76].

Most patients with COVID-19 are asymptomatic or experience only mild symptoms, including fever, dry cough, and shortness of breath. However, some individuals deteriorate rapidly and develop ARDS. The most common histopathologic correlate of ARDS is diffuse alveolar damage (DAD), characterized by hyaline membrane formation in the alveoli in the acute stage, and interstitial widening by edema and fibroblast proliferation in the organizing stage. Barton and colleagues reported that DAD has a long list of potential etiologies, including infection, vaping-associated pulmonary injury, oxygen toxicity, drug toxicity, toxic inhalants or ingestants, shock, severe trauma, sepsis, irradiation, and acute exacerbations of usual interstitial pneumonia [77].

Schaller et al., 2020 recent report of examinations conducted in Germany states that "because there are still insufficient data on cause of death, we describe postmortem examinations in a case series of patients with COVID-19" [78]. Between April 4 and April 19, 2020, the serial postmortem examinations were conducted in patients with proven severe acute respiratory syndrome coronavirus 2 (SARS-CoV-2) infection who died at the University Medical Center Augsburg (Germany). Autopsies were conducted according to published best practice. Specimens from lung, heart, liver, spleen, kidney, brain, pleural effusion, and cerebrospinal fluid (CSF) were assessed. Postmortem nasopharyngeal, tracheal, bronchial swabs, pleural effusion, and CSF were tested for SARS-CoV-2 by reverse transcriptase–polymerase chain reaction. In this postmortem evaluation of 10 patients with COVID-19, acute and organizing diffuse alveolar damage and SARS-CoV-2 persistence in the respiratory tract were the predominant histopathologic findings and constituted the leading cause of death in patients with and without invasive ventilation. Periportal liver lymphocyte infiltration was considered unspecific inflammation. Whether myoepicardial alterations represented systemic inflammation or early myocarditis is unclear; criteria for true myocarditis were not met. Central nervous system involvement by COVID-19 could not be detected. This study has limitations, including the small number of cases from a single center and missing proof of direct viral organ infection [78].

Pulmonary postmortem findings in a series of COVID-19 cases were revealed in northern Italy two-center descriptive study [79]. The predominant pattern of lung lesions in patients with COVID-19 patients is diffuse alveolar damage, as described in patients infected with severe acute respiratory syndrome and Middle East respiratory syndrome coronaviruses. Hyaline membrane formation and pneumocyte atypical hyperplasia are frequent. Importantly, the presence of platelet–fibrin thrombi in small arterial vessels is consistent with coagulopathy, which appears to be common in patients with COVID-19 [79].

Tyramine infusion in twelve healthy active males causes a local noradrenaline release in the leg. The increase in noradrenaline was associated with an increase in clot microstructure formation [80]. Biogenic amines tyramine, tryptamine and β-phenyletylamine are secondary metabolites of microbial shikimate pathway produced by human microbiome [1, 2].

In China reports, COVID-19, caused by severe acute respiratory syndrome coronavirus 2 (SARS-CoV-2) infection, is associated with coagulopathy causing venous and arterial thrombosis [81, 82]. Recent data from the pandemic epicenter in Wuhan, China, reported neurological complications in 36% of 214 patients with COVID-19; acute cerebrovascular disease (mainly ischemic stroke) was more common among 88 patients with severe COVID-19 than those with non-severe disease (5.7% versus 0.8%) [83].

However, the mechanisms, phenotype, and optimal management of ischemic stroke associated with COVID-19 remain uncertain [84]. Beyrouti and other researchers in London, UK described the demographic, clinical, radiological, and laboratory characteristics of six consecutive patients assessed April 1–16, 2020 at the National Hospital for Neurology and Neurosurgery, Queen Square, London, UK, with acute ischemic stroke and COVID-19 (confirmed by reverse-transcriptase PCR (RT-PCR)). All six patients had large vessel occlusion with markedly elevated D-dimer levels ($\geq 1000\,\mu g/L$). Three patients had multiterritory infarcts, two had concurrent venous thrombosis, and, in two, ischemic strokes occurred despite therapeutic anticoagulation [84].

In New Orleans, autopsies were performed on ten African American decedents aged 44–78 years with cause of death attributed to COVID-19, reflective of the dominant demographic of deaths following COVID-19 diagnosis [85]. Important findings include the presence of thrombosis and microangiopathy in the small vessels and capillaries of the lungs, with associated hemorrhage, that contributed to death. Features of diffuse alveolar damage, including hyaline membranes, were present, even in patients who had not been ventilated. Cardiac findings included individual cell necrosis without lymphocytic myocarditis. There was no evidence of secondary pulmonary infection by microorganisms [85].

Solomon et al. [86] reported that neurologic symptoms, including headache, altered mental status, and anosmia, occur in many patients with COVID-19. The neuropathological findings were from autopsies of 18 consecutive patients with SARS-CoV-2 infection who died in a single teaching hospital between April 14 and April 29, 2020 in Massachusetts, USA [86]. All the patients had nasopharyngeal swab samples that were positive for SARS-CoV-2 on qualitative reverse-transcriptase–polymerase-chain-reaction (RT-PCR) assays. Histopathological examination of brain specimens obtained from 18 patients who died 0 to 32 days after the onset of symptoms of COVID-19 showed only hypoxic changes and did not show encephalitis or other specific brain changes referable to the virus. The virus was detected at low levels in six brain sections obtained from 5 patients; these levels were not consistently related to the interval from the onset of symptoms to death. Positive tests may have been due to *in situ* virions or viral RNA from blood [86].

The autopsy findings of 21 COVID-19 patients hospitalized at the University Hospital Basel and at the Cantonal Hospital Baselland, Switzerland were reported by Menter et al. [87]. The primary cause of death was respiratory failure with exudative diffuse alveolar damage and massive capillary congestion, often accompanied by microthrombi despite anticoagulation. Ten cases showed superimposed bronchopneumonia. Further findings included pulmonary embolism ($n = 4$), alveolar hemorrhage ($n = 3$), and vasculitis ($n = 1$). Pathologies in other organ systems were predominantly attributable to shock; three patients showed signs of generalized and five of pulmonary thrombotic microangiopathy. Six patients were diagnosed with senile cardiac amyloidosis upon autopsy. Most patients suffered from one or more comorbidities (hypertension, obesity, cardiovascular diseases, and diabetes mellitus). Additionally, there was an overall predominance of males and individuals with blood group A (81% and 65%, respectively) [87]. Myocardial hypertrophy observed in 71% COVID-19 cases Liver pathologies such as liver steatosis was observed in 41% and liver shock necrosis in 29% of COVID-19 cases. The cytoplasm of kidney podocytes, endothelial cells and proximal tubular epithelial cells contained multiple vesicles revealed by electron microscopy [87]. At higher magnification, the vesicles contain double membranes. Similar multiple vesicles were earlier observed in AD brain and in tryptamine-treated human neuronal cells by Paley [4]. In summary, the findings provide an insight into the complexity of COVID-19 pathophysiology. SARS-CoV-2 substantially contributed to fatality in all cases, but the authors postulate a

multifactorial cause of death, with COVID-19 as a contributory factor in multimorbid patients [87]. Major findings that imply an impaired microcirculation include pulmonary capillarostasis and the presence of microthrombi in the lungs and kidneys despite anticoagulation. The findings corroborate clinical and epidemiological data on cardiovascular morbidity and disease outcome and add amyloid transthyretin (ATTR) amyloidosis as a risk factor. Of note, ATTR is thyroxine-binding prealbumin while serum thyroxine was lower in severe COVID-19 compared to nonsevere cases and healthy individuals [23].

Barton et al. (2020) report the findings of two complete autopsies of severe acute respiratory syndrome coronavirus 2 (SARS-CoV-2) positive individuals who died in Oklahoma in March 2020 [77]. A 77-year-old obese man with a history of hypertension, splenectomy, and 6 days of fever and chills died while being transported for medical care. He tested positive for SARS-CoV-2 on postmortem nasopharyngeal and lung parenchymal swabs. Autopsy revealed diffuse alveolar damage, chronic inflammation, and edema in the bronchial mucosa. A 42-year-old obese man with a history of myotonic dystrophy developed abdominal pain followed by fever, shortness of breath, and cough. Postmortem nasopharyngeal swab was positive for SARS-CoV-2; lung parenchymal swabs were negative. Autopsy showed acute bronchopneumonia with evidence of aspiration. Neither autopsy revealed viral inclusions, mucus plugging in airways, eosinophils, or myocarditis [77]. Bacterial cultures (aerobic/anaerobic) of the lung tissue from the 42-year-old patient grew nontoxigenic *Escherichia coli*, *Candida tropicalis*, and *Proteus mirabilis*. In complete autopsy of the 77-year-old patient, the hepatic centrilobular steatosis and remote cholecystectomy and in the 42-year-old, hepatic cirrhosis and advanced remote cholecystectomy were revealed. Coronary artery disease was found in both patients.

Ackermann et al. reported in 2020 that the lungs from patients with COVID-19 showed distinctive vascular features, consisting of severe endothelial injury associated with the presence of intracellular virus and disrupted cell membranes. Histologic analysis of pulmonary vessels in patients with COVID-19 showed widespread thrombosis with microangiopathy. Alveolar capillary microthrombi were 9 times as prevalent in patients with COVID-19 as in patients with influenza ($p < 0.001$). In lungs from patients with COVID-19, the amount of new vessel growth— predominantly through a mechanism of intussusceptive angiogenesis—was 2.7 times as high as that in the lungs from patients with influenza ($p < 0.001$) [88]. In this study, pulmonary autopsy specimens from seven patients who died from respiratory failure caused by SARS-CoV-2 infection were compared with lungs from seven patients who died from pneumonia caused by influenza A virus subtype H1N1—a strain associated with the 1918 and 2009 influenza pandemics [88].

Archer et al. described in 2020 the differences between COVID-19 pneumonia, acute respiratory distress syndrome, and high altitude pulmonary edema (HAPE) [89]. Although 80% of people with COVID-19 have a minor, acute respiratory infection, the mortality ranges from 2% to 7%. Patients with COVID-19 pneumonia may decompensate because of hypoxemic respiratory failure. Autopsy data show inflammation, diffuse alveolar damage, alveolar fluid accumulation, and occasional hyaline membranes, consistent ARDS [89]. Recently, HAPE physiology was proposed to explain the edema and hypoxemia in COVID-19 pneumonia.

Fried et al reported 4 cases (positive SARS-CoV-2 testing) that illustrate a variety of cardiovascular presentations of COVID-19 infection [90]. *Case 1:* A 64-year-old woman is presented with COVID-19 pneumonia and differential diagnosis included myopericarditis and cardiac amyloidosis. *Case 2:* A 38-year-old man with a history of type 2 diabetes mellitus presented with 1 week of cough, pleuritic chest pain, and progressive shortness of breath to an outside hospital. The patient had a bradycardic arrest lasting 6 minutes. *Case 3:* A 64-year-old woman with a nonischemic cardiomyopathy, atrial fibrillation, hypertension, and diabetes mellitus presented with a nonproductive cough and shortness of breath for 2 days. On arrival, she was afebrile, with blood pressure 153/120 mm Hg, heart rate 100 bpm, and oxygen saturation 88%. *Case 4:* A 51-year-old man with a history of heart transplantation in 2007 and renal transplantation in 2010 presented with intermittent fever, dry cough, and shortness of breath for 9 days. He denied any recent travel or sick contacts. His outpatient immunosuppression included tacrolimus 5 mg twice daily, mycophenolate mofetil 250 mg twice daily, and prednisone 5 mg daily [90].

In our study, the congophilic cerebral angiopathy associated with angiogenesis was revealed in blood vessels of tryptamine-treated mouse [91]. Thus two biogenic amines produced by human gut microbiome tryptamine [91] and tyramine [80] can induce thrombosis, microangiopathy and angiogenesis similar to

those revealed in COVID-19 patients [77, 79, 84, 85, 88].

Pneumonia in elderly before COVID-19 era

Cacciatore et al. (2017) presented analysis of Italian cases of pneumonia observed in elderly [92] before COVID-19 was discovered. The data of this study are suitable for comparison with pneumonia associated with COVID-19 positivity. The authors discuss several important aspects of pneumonia in the elderly, which is a common and severe problem. In this review, the authors analyze the state of the art for pneumonia in the elderly. Several aspects are discussed: 1) how common is the disease; signs and symptoms in the elderly; 2) the elderly must always be hospitalized and which is the best place - ICU or medical ward?; 3) the role of comorbidities; 4) etiology and pathogenesis; medical treatment - when and how to start; 5) antibiotic resistance; 6) antibiotics in hospital-acquired and ventilator-related pneumonia; 7) assisted non-invasive ventilation; 8) the treatment in the terminally ill elderly patient [92]. Pneumonia is a frequent illness highly conditioning morbidity and mortality in the elderly population. In this age group, similarly, in all racial groups, it is the fourth leading cause of death and the leading cause of death from infectious disease. Pneumonia often is the terminal event that complicates a long-term illness (dementia, cancer, as prolonged immobilization syndrome). Authors distinguish different types of pneumonia depending on the environment in which they develop: community acquired pneumonia (CAP) or pneumonia community, nursing home acquired pneumonia or hospital acquired pneumonia or in hospital development and ventilator-associated pneumonia [92]. Data derived from an observational study conducted by the authors in the Emergency Department of Cardarelli Hospital in Naples, between January 1, 2015 and October 15, 2015, identified 3,255 patients with respiratory infection diagnosis on 72,134 accesses to the Emergency Department. The incident rate of respiratory infection is 45/1,000 patients of which 1,559/72,134 corresponding to an incidence rate of 22/1,000 with a diagnosis of pneumonia, increasing to 77.4/1,000 for patients with 65 years and over. In elderly patients hospitalized for pneumonia, the mortality rate is about 20%. If pneumonia develops in patients already hospitalized for other conditions, mortality increase to 50–70%, and is higher in women than in men. Pneumonia is the most common form of hospital-acquired infection. Data from European Center Disease Control (ECDC), published in 2015, related to a survey conducted on 231,459 patients hospitalized between 2011 and 2012, identified 13829 patients (6.0%) with hospital infection [92]. For comparison, the estimated COVID-19 positive is 8.408% in Florida currently and 0.36% COVID-19 positive were hospitalized residents of total Florida population.

Therefore, the incidence of COVID-19-related pneumonia from March 2020 to February 2021 in Florida is essentially lower than the incidence of pneumonia in Europe in the period before COVID-19.

Jackson et al. reported in 2004 [93] that the overall rate of community-acquired pneumonia ranged from 18.2 cases per 1,000 person-years among persons aged 65–69 years to 52.3 cases per 1,000 person-years among those aged ≥85 years. In this US population, 59.3% of all pneumonia episodes were treated on an outpatient basis. In multivariate analysis, risk factors for community-acquired pneumonia included age, male sex, chronic obstructive pulmonary disease, asthma, diabetes mellitus, congestive heart failure, and smoking. On the basis of these data, the authors estimate that roughly 915,900 cases of community-acquired pneumonia occur annually among seniors in the US and that approximately 1 of every 20 persons aged > or = 85 years will have a new episode of community-acquired pneumonia each year [93].

CDC estimates that influenza was associated with more than 35.5 million illnesses, more than 16.5 million medical visits, 490,600 hospitalizations, and 34,200 deaths during the 2018–2019 influenza season. This burden was similar to estimated burden during the 2012–2013 influenza season (Centers for Disease C, Prevention. Estimated influenza illnesses and hospitalizations averted by influenza vaccination – United States, 2012–13 influenza season. MMWR Morb Mortal Wkly Rep 2013; 62(49): 997–1000).

Other necrotizing infections

It was discussed here that COVID-19 positivity can be associated with necrotizing pneumonia [49]. Moreover, cardiac necrosis [85] and liver shock necrosis [87] were found in COVID-19 patients. Thereby, the other necrotizing medical conditions can be related to necrosis in different organs of COVID-19 patients.

Erichsen Andersson et al. presented in 2018 the analysis of necrotizing fasciitis (NF) experienced by survivors and family in Nordic multi-center study [94]. Necrotizing soft tissue infection is the most serious of all soft tissue infections. The patient's life is dependent on prompt diagnosis and aggressive

treatment. Diagnostic delays are related to increased morbidity and mortality, and the risk of under- or missed diagnosis is high due to the rarity of the condition [94].

Molecular characterization of methicillin-resistant *Staphylococcus aureus* from a fatal case of NF in an extremely low-birth-weight infant was characterized by Orii et al. (2010) in Japan [95].

Peker et al reported (2010) a case of invasive and mortal NF caused by *Staphylococcus epidermidis* in an infant with extremely low birthweight in Turkey [96].

The case of multifocal NF complicating a single vaccine injection was reported by Perbet et al. in France [97]. Injection of hepatitis B vaccine of a 16-year-old immunocompetent woman developed into rapidly spreading multifocal NF of the right arm and the thighs, with septic shock. Treatment with antimicrobial therapy and surgical debridements allowed amputation to be avoided with a favourable outcome. The etiological agent was a methicillin-sensitive *Staphylococcus aureus* isolate [97].

The complete genome sequence of a highly virulent methicillin-sensitive *Staphylococcus aureus* strain, MCRF184, belonging to sequence type 45 was reported by Aswani et al. (2016) [98]. This staphylococcal strain was isolated in Wisconsin, USA from a surgical biopsy specimen of a patient with necrotizing fasciitis [98].

One of most recent case of necrotizing enterocolitis, medical condition that lead to premature birth was recently reported by Kim and Seo (2020) [99].

Challenges in diagnosing necrotizing enterocolitis were outlined in another report (2020) [100]. *Staphylococcus* is related to necrotizing enterocolitis. Particularly, necrotizing enterocolitis with epidemic Staphylococcus in a neonatal intensive care unit was reported in 1984 [101]. In 2012, Lemyre et al. [102] reported that a decrease in the number of cases of necrotizing enterocolitis is associated with the enhancement of infection prevention. This report describes control measures during a *Staphylococcus aureus* outbreak in a neonatal intensive care unit (2012) [102].

The severity of acute necrotizing pancreatitis ranges from self-limited to rapidly progressive illness leading to multiple organ failure. Ala-Kokko et al. of Oulu University Hospital, Finland reported that *Staphylococcus epidermidis* in pancreatic necrosis was associated with increased mortality in the study of 67 consecutive patients [24]. Mechanical ventilation ($p = 0.002$), surgical management ($p = 0.028$), open packing surgical management ($p = 0.03$), renal replacement therapy ($p < 0.001$), use of inotropic drugs ($p = 0.012$), and *Staphylococcus epidermidis* growth ($p = 0.029$) in infected pancreatic tissue were all associated with mortality [24]. While most complicating infections in animal pancreatic studies, hospitalized patients, and in pancreatic infection are caused by a few species of bacteria, normal intestinal flora consists of more than 400 species. In the natural course of severe acute pancreatitis, cultures of infected pancreatic necroses yield monomicrobial flora in 60–87% of cases; in these studies, polymicrobial flora was confirmed in only 13–40% of cases. A preponderance of Gram negative aerobic bacteria is usually present (*Escherichia coli*, *Pseudomonas* spp, *Proteus*, *Klebsiella* spp) which suggests an enteric origin, but Gram positive bacteria (*Staphylococcus aureus*, *Streptococcus faecalis*, *Enterococcus*), anaerobes, and, occasionally, fungi have also been found [103].

A short temporal history of pancreatitis was highly associated with pancreatic cancer in analysis of the data from two pooled case-control studies of pancreatic cancer ($n = 4,515$) in the San Francisco Bay Area and the M.D. Anderson Cancer Center, suggesting that pancreatitis may be an early manifestation of pancreatic cancer in some individuals [104]. Acute pancreatitis is linked to pancreatic cancer. Sadr-Azodi et al. (2018) reported a population-based cohort study including all Swedish residents diagnosed with a first-time episode of acute pancreatitis between 1997 and 2013 and corresponding matched pancreatitis-free individuals from the general population [105]. Overall, 49,749 individuals with acute pancreatitis and 138,750 matched individuals without acute pancreatitis were followed up for 1,192,134 person-years (median 5.3 years). A total of 769 individuals developed pancreatic cancer, of whom 536 (69.7%) had a history of acute pancreatitis. The risk of pancreatic cancer was substantially increased during the first few years after a diagnosis of acute pancreatitis but declined gradually over time, reaching a level comparable to the pancreatitis-free population after > 10 years of follow-up. In those with non-gallstone-related acute pancreatitis, the risk of pancreatic cancer declined to a level comparable to the pancreatitis-free population only when follow-up time was censored for a second episode of acute pancreatitis or a diagnosis of chronic pancreatitis. Increasing number of recurrent episodes of acute pancreatitis was associated with increased risk of pancreatic cancer. These findings imply a delay in the

diagnosis of pre-existing pancreatic cancer, if clinically presented as acute pancreatitis. Any association between non-gallstone-related acute pancreatitis and pancreatic cancer in the long-term (> 10 years) could be mediated through recurrent acute pancreatitis or chronic pancreatitis [105].

Case of fatal myocardial necrosis caused by *Staphylococcus lugdunensis* and Cytomegalovirus in a patient with scleroderma was reported by Pirilä et al. in Finland (2006) [106]. At the autopsy extensive necrosis of the myocardium was seen, with an almost complete absence of inflammatory cells and the presence of bacterial structures identified as *Staphylococcus lugdunensis* by PCR.

Paley (2021) [2] suggests that tryptamine, an inducer of necrosis and a metabolic product of some *Staphylococcus* strains, can be implicated in necrotizing diseases such as necrotizing pneumonia. Here I discuss other necrotizing diseases and medical conditions: necrotizing fasciitis, necrotizing enterocolitis, necrotizing pancreatitis and myocardial necrosis in connection with community-acquired or hospital-acquired (nosocomial) *Staphylococcus* infections in different countries. I recommend the measurement of necrosis-inducing tryptamine and other biogenic amines for characterization of bacterial clinical isolates especially from cases of necrotizing diseases and conditions.

Coagulase-negative staphylococci (CNS) are the predominant bacteria found in fermented foods worldwide. Because of this, food-derived CNS are used as starters for cheese and meat fermentation, and have been investigated for use as starters in soybean fermentation. Although food-derived CNS are generally considered non-pathogenic, their safety remains uncertain following the isolation of CNS from skin infections in humans and animals, and because they belong to the same genus as the highly pathogenic species *Staphylococcus aureus*. The food-derived CNS produce tryptamine and other biogenic amines [107].

Taken together the data support that SARS-CoV-2 can be a contributory factor in all cases with COVID-19 of a multifactorial cause of death in multimorbid patients.

Bacteria and virus interactions in influenza

Bacteria and viruses interact in infectious diseases. The interaction can result from viral activation of opportunistic bacteria as suggested by studies or bacteria can interact with virus upon infection in other studies. Both COVID-19 virus positivity and associated pneumonia resolved following anti-bacterial treatment with antibiotic in some cases. Accumulating evidence implicates metabolites produced by gut microbes as crucial mediators of diet-induced host-microbial cross-talk. Some bacteria produce tryptamine and other biogenic amines as I described in a previous review [1]; therefore these are not discussed in details here. One can assume that biogenic amines produced by human microbiome can play a role in viral infections. Here I review the virus-bacteria interaction and a role of microbial biogenic amines in this interaction.

Otitis media (OM) is one of the most common childhood diseases. OM can arise when a viral infection enables bacteria to disseminate from the nasopharynx to the middle ear. In the study conducted by Short et al, 2011, mice coinfected with *Streptococcus pneumoniae* and influenza virus had high bacterial load in the middle ear, middle ear inflammation, and hearing loss. In contrast, mice colonized with *S. pneumoniae* alone had less bacteria in the ear, minimal hearing loss, and no inflammation. Of interest, infection with influenza virus alone also caused some middle ear inflammation and hearing loss. Influenza virus alone causes middle ear inflammation in infant mice. This inflammation may then play an important role in the development of bacterial OM [108].

Epidemiological observations and animal models have long shown synergy between influenza virus infections and bacterial infections. Influenza virus infection leads to an increase in both the susceptibility to secondary bacterial infections and the severity of the bacterial infections, primarily pneumonias caused by *Streptococcus pneumoniae* or *Staphylococcus aureus*. Rowe et al., 2019 showed that, in addition to the widely described immune modulation and tissue-remodeling mechanisms of bacterial–viral synergy, the virus interacts directly with the bacterial surface. Similar to the recent observation of direct interactions between enteric bacteria and enteric viruses, the authors observed a direct interaction between influenza virus on the surface of Gram-positive, *S. pneumoniae* and *S. aureus*, and Gram-negative, *Moraxella catarrhalis* and non-typeable *Haemophilus influenzae*, bacterial colonizers and pathogens in the respiratory tract. Pre-incubation of influenza virus with bacteria, followed by the removal of unbound virus, increased bacterial adherence to respiratory epithelial cells in culture. This result was recapitulated

in vivo, with higher bacterial burdens in murine tissues when infected with pneumococci pre-incubated with influenza virus versus control bacteria without virus. These observations support an additional mechanism of bacteria–influenza virus synergy at the earliest steps of pathogenesis [109].

The sadA-expressing staphylococci showed increased adherence to human colorectal adenocarcinoma HT-29 cells and 2- to 3-fold increased internalization. Internalization and adherence was also increased in a sadA mutant in the presence of tryptamine [17, 18]. Treating *S. aureus* USA300 with biogenic amines serotonin and tryptamine increased internalization by approximately threefold [18].

It is suggested that tryptamine acts by loosening the tightly packed DNA in bacteriophage heads, whereas putrescine stabilizes it [110]. This way biogenic amines can affect the bacteria survival. .

Thus the biogenic amine increase adherence of Staphylococcus to human cells [17, 18] whereas virus increased bacterial adherence to respiratory epithelial cells in culture [109].

Taken together these observations support an additional mechanism of bacteria–virus-biogenic amine synergy at the earliest steps of pathogenesis.

Autoantigenome

An autoantigenome by dermatan sulfate affinity from human lung HFL1 cells was reported recently in 2021 by Wang et al. [111]. The authors suggest that an autoantigen atlas may explain neurological and autoimmune manifestations of COVID-19. The six cytoplasmic aminoacyl-tRNA synthetases (ARS) including tryptophanyl-tRNA synthetase (TrpRS or WARS), alanyl-tRNA synthetase (AARS), bifunctional glutamyl-prolyl-tRNA synthetase (EPRS1), histidyl-tRNA synthetase, lysyl-tRNA synthetase and glutaminyl-tRNA synthetase (GlnRS) showed affinity to dermatan sulfate (DS) while such DS affinity is a feature of autoantigens [111]. Earlier we demonstrated that TrpRS is a human autoantigen detected in human sera by ELISA and immunoblotting with prevalence in cancer patients [10]. TrpRS is secreted from human macrophages, fibroblasts, and endothelial cells in response to the proinflammatory cytokine interferon gamma (IFNgamma) [112]. Zhou et al. (2020) review the roles of aminoacyl-tRNA synthetases in cancer [113]. The three ARS (AARS, EPRS, WARS) autoantigens are altered in COVID-19 [111]. Glyceraldehyde-3-phosphate dehydrogenase (GAPDH) and Rab GDP dissociation inhibitor alpha

(GDI1), the autoantigens reveled by dermatan sulfate affinity are COVID-altered [111]. GAPDH [114], GDI1 [1] and glutamyl-tRNA synthetase (GluRS) [9] are TrpRS bound proteins. Analysis of COVID-altered proteins revealed a strong link to the nervous system. Of the 352 COVID-altered proteins, at least 150 are related to the nervous system. TrpRS plays a role in the viral infections [115, 116].

Using dermatan sulfate (DS) affinity enrichment of autoantigenic proteins extracted from HS-Sultan lymphoblasts, Wang et al. [117] identified 362 DS-affinity proteins, of which at least 201 (56%) are confirmed autoantigens including cytoplasmic tryptophanyl-tRNA synthetase [10] altered (up and/or down) in COVID-19 [117].

Metabolomics in COVID-19 and non-COVID-19 patients, and healthy controls

Some shikimate pathway metabolites found to be altered in sera of non-severe COVID-19, severe COVID-19 and non-COVID-19 patients with dysregulation of macrophage, platelet degranulation, complement system pathways, and massive metabolic suppression in comparison with healthy individuals. These and other sera metabolites were recently reported in the study conducted by Shen and colleagues in China [23]. I selected the metabolites related to microbial shikimate pathway in human sera and summarized in Table 2.

This study highlights dysregulation of multiple immune and metabolic components in clinically severe patients [23]. Human serum benzoate is statistically significantly higher in severe-COVID-19, non-severe COVID-19, and non-COVID-19 patients in comparison with healthy individuals while no difference reveled between severe and non-severe COVID-19 patients (Table 2). Zinc benzoate, a contaminating environmental compound inhibits monoamine oxidase type A [120].

Shikimate pathway metabolite benzoate and its metabolite, hippurate, are altered in a number of medical conditions and diseases (Table 3). Particularly, hippurate increased in plasma of patients with AD [121] and decreased in sera of patients with severe COVID-19 [121].

Alteration of tryptophan metabolism in sera of COVID-19–positive patients was observed in metabolomics study conducted by Thomas et al. [132]. In this study, subjects seen at New York-Presbyterian/Columbia University Irving Medical Center included 33 COVID-19–positive patients, as

determined by SARS-CoV-2 nucleic acid testing of nasopharyngeal swabs. The control group included 16 subjects. Tryptophan metabolism was the top pathway affected by COVID-19 in the analysis of targeted and untargeted metabolomics data. As such, focused analysis of this pathway highlighted decreases in tryptophan, serotonin, and indolepyruvate levels. In contrast, increases in kynurenine, kynurenic acid, picolinic acid, and nicotinic acid, but not anthranilate, suggested hyperactivation of the kynurenine pathway. Tryptamine pathway was highlighted in untargeted metabolomics analyses.

Therefore tryptophan metabolism was identified in targeted and untargeted metabolomics data as the top pathway affected by COVID-19. In particular, decreases in tryptophan and increases in kynurenine were proportional to disease severity [132].

Metabolic pathway analysis of COVID-19-altered fecal metabolites includes validated data on aminoacyl-tRNA biosynthesis and biosynthesis of aromatic amino acids, the products of shikimate pathway tryptophan, phenylalanine and tyrosine in the Chinese study by Lv et al. [133].

Recently, with the use of liquid-chromatography/gas chromatography mass spectrometry metabolomics profiling, Wu et al. [134] identified statistically significant differences ($p < 0.001$) between AD and healthy controls for gut microbial tryptophan metabolites, short-chain fatty acids, and lithocholic acid, the majority of which correlated with altered microbiota and cognitive impairment. The fecal indole-3-pyruvic acid was 21.021-fold higher in AD than in healthy controls [134]. Tryptophan can be converted to the plant hormone auxin indole-3-acetic acid (IAA) via indole-3-pyrivic acid or via tryptamine [135]. Tryptamine, indole-3-pyruvic acid and IAA are all inhibitors of TrpRS [91] and thus these tryptophan metabolites can interfere with protein biosynthesis causing disease [1]. A 2-fold helix is formed between the molecules of tryptamine and acid through salt interaction and hydrogen bonding in the lattice. The torsional ethylamino group of the tryptamine molecule and the carboxylic acid group play an important role in producing this helical structure. Tryptamine form a 2-fold helix with IAA [136, 137].

In 2013, Kaddurah-Daouk et al. reported the targeted metabolomics profiling of CSF)from AD, mild cognitive impairment (MCI), and control subjects. The findings indicate that MCI and AD are associated with an overlapping pattern of perturbations in tryptophan, tyrosine, methionine, and purine pathways [138]. Tryptamine metabolite IAA was higher

~1.41-fold ($p = 0.02$) in MCI (mean 139.11) versus controls (mean 98.40) [138]. In addition, IAA/tryptophan ratio was ~1.35-fold higher ($p = 0.01$) in MCI versus controls [138]. Although Kaddurah-Daouk et al. [138] had not cited our studies on tryptamine-induced neurodegeneration, the work of these authors supports our AD-like model of tryptamine-induced neurodegeneration [3, 4, 91, 139, 140] and a concept of protein biosynthesis interference in disease based on this model [1].

Thus, both age-dependent diseases AD and COVID-19 are linked to alterations in tryptophan metabolism. The tryptophan metabolites can form helixes [136, 137] while histological manifestations show helical inclusions in human AD brain [4, 9] and in tryptamine-treated cell and mouse models [3].

Biogenic amines: How to reduce the dose-dependent toxicity and anti-cancer effect

By definition, biogenic amines are basic nitrogenous compounds formed mainly by decarboxylation of amino acids. Biogenic amines such as histamine, tyramine, and putrescine play an important role in many critical functions in man and animals [141]. Tryptamine (at $500\,\mu M$ and $1\,mM$) and other indoleamines tryptophan and serotonin bind to main histopathological structures of AD plaques and tangles in AD human brain autopsy thus reducing binding of substrates of cholinesterases - acetylcholine and butyrylcholine to these structures [142]. Acetylthiocholine was used as the substrate for the acetylcholinesterase (AChE) reaction, and butyrylthiocholine was used for the butyrylcholinesterase (BChE) reaction, each at $366\,\mu M$ [142]. Thus, tryptamine is able to compete *in situ* with cholinesterases's substrates at similar concentrations. Neurofibrillary tangles and amyloid plaques express acetylcholinesterase and butyrylcholinesterase activity in AD [142] while tryptamine is inhibitor of cholinesterases [2]. None of tyrosine, tyramine or glycine (1 mM each) were able to compete with AChE and BChE substrates *in situ* in AD neurofibrillary tangles and plaques [142]. Cholinesterase activity releases a reaction product choline whereas serum choline and choline metabolites are statistically significantly reduced in COVID-19 patients in metabolomics study [23]. Tryptophan and serotonin are also reduced in sera of COVID-19 patients. Butyrate in the active site of human BChE has been modeled as bound butyrate in the BChE crystal structure [143] while butyrate metabolites are

altered in sera of COVID-19 patients [23]. For instance, the 3-hydroxybutyrate (BHBA) increased 2.2-fold ($p = 0.0013$) in severe COVID-19 patients (65 patients who visited Taizhou Hospital, China from January to March 2020) compared to healthy controls (28 healthy individuals). 3-hydroxybutyrate (BHBA) is higher 3.14-fold ($p = 9.67–06$) in non-COVID-19 patients (25 non-COVID-19 patients with similar clinical characteristics including fever and/or cough as COVID-19 patients however negative in the nucleic acid test) compared to healthy control [23]. The level of β-hydroxybutyrate (β-hydroxybutyric acid, also known as 3-hydroxybutyric acid) decreased in AD patients, and donepezil, a first-line acetyl-cholinesterase inhibitor used for the treatment of AD elevated the plasma level of β-hydroxybutyrate. Donepezil increased the plasma and liver levels of β-hydroxybutyrate in mice [144].

The 3-hydroxybutyrate (BHBA) is higher in Oklahoma native American Indian population (C&A) with a high rate of obesity and diabetes [145]. Particularly, I estimated that in non-native control population the high levels of fecal BHBA is in 4.347% of population and in C&A-17.1% of population. The C&A population have a high prevalence of AD associated gut bacteria [7, 8].

BHBA is an endogenous inhibitor of histone deacetylases and a ligand for at least two cell surface receptors. In addition, the downstream products of BHBA metabolism including acetyl-CoA, succinyl-CoA, and NAD + (nicotinamide adenine dinucleotide) themselves have signaling activities. These regulatory functions of BHBA serve to link the outside environment to cellular function and gene expression, and have important implications for the pathogenesis and treatment of metabolic diseases including type 2 diabetes [146].

Altogether, these data support suggestion that cholinesterase activity can be inhibited in blood of both COVID-19 and non-COVID-19 patients of the same study conducted in China. Pneumonia was shown to be a risk factor for death in patients (the medical records of 155 patients) with cholinesterase inhibitor poisoning in central Taiwan, from January 2002 to December 2004 [147].

The degree of BHBA elevation with hyperglycemic emergencies has been well characterized, with BHBA level >3 mmol/L in children or >3.8 mmol/L in adults being presumptive evidence of diabetic ketoacidosis. Normally, circulating BHBA levels are below 0.5 mmol/L, but with starvation, levels can rise up to 6 mmol/L [148].

Hyperketonemia is defined as BHBA ≥ 1 mmol/L, in the absence of a diagnosis of diabetic ketoacidosis or/and hyperglycemic hyperosmolar syndrome [148]. Complications of the brain, kidney, liver, and microvasculature were found to be elevated in diabetic patients who had elevated ketones compared to those diabetics with normal ketone levels [149].

Therefore, consumption of food containing high amounts of the biogenic amines and production of high amounts of biogenic amines by human microbiome may have deleterious effect on human health. The micromolar concentrations of tryptamine were detected in humans and other mammals [1]. For instance, concentration of tryptamine in colonic contents (μM) was 33.7 (SEM 8.5) in horses (N = 10) [150]. Taking into account that biogenic amines result from enzymatic activity of the food or bacteria with active decarboxylase, control or inhibition of such processes and prevention of bacterial growth are key factors fundamental for limiting the amine content in food. It was demonstrated by Takaki [151] that after superfusion at high concentration, tryptamine initially acted like serotonin, but then blocked the action of serotonin on these cells. Measurements of the release of preloaded [3H]serotonin or [3H]norepinephrine revealed that tryptamine is a potent releaser of these labeled amines; this release is Ca2 + independent but temperature dependent. Moreover, incubation with tryptamine depleted the myenteric plexus of endogenous serotonin [151]. Tryptamine produced a slow hyperpolarization in a few neurons other than a slow depolarization in myenteric neurons of the isolated guinea-pig ileum [152]. The conformational space of tryptamine has been thoroughly investigated using rotationally resolved laser-induced fluorescence spectroscopy.

Six conformers could be identified on the basis of the inertial parameters of several deuterated isotopomers. Upon attaching a single water molecule, the conformational space collapses into a single conformer. For the hydrogen-bonded water cluster, this conformer is identified unambiguously as tryptamine A. In the complex, the water molecule acts as proton donor with respect to the amino group. An additional interaction with one of the aromatic C–H bonds selectively stabilizes the observed conformer more than all other conformers. Ab initio calculations confirm much larger energy differences between the conformers of the water complex than between those of the monomers [153].

Medina et al. (2003) reported that biogenic amines (arginine/ornithine-derived polyamines might also be

considered biogenic amines) are ubiquitous in localization (in fact, they are present in almost every kind of cell) and have pleiotropic effects, with a recognized major role as essential compounds in maintaining macromolecular synthesis and cell proliferation rates [154]. The properties of histamine are discussed in Hellstrand review (2002) in relation to the current use of histamine as an adjunct to IL-2 in metastatic melanoma and other malignant diseases [155]. In 1997, Hellstrand et al. [156] reported that more than 50 patients with neoplastic disease have been treated with histamine, given in subcutaneous injections, together with IL-2 or IFN-alpha. The results of two pilot trials in metastatic melanoma suggest that the addition of histamine to IL-2 and IFN-alpha prolongs survival time and induces regression of tumors, such as liver melanoma, which are otherwise considered refractory to immunotherapy. The results of a trial in acute myelogenous leukemia (AML) suggest that histamine and IL-2 protects AML patients against relapse of leukemic disease. Histamine is well tolerated: for example, AML patients in remission have treated themselves with histamine at home without supervision for a total of >300 weeks with only a handful of therapy-related hospital contacts [156].

Biogenic amines in the flesh of sailfish (*Istiophorus plafypferus*) was shown to be responsible for scornbroid poisoning [157]. An incident of food poisoning due to ingesting the flesh of sailfish occurred in Changhua Prefecture, western Taiwan, in July 1994. The incident caused illness of 12 victims from five families. Symptoms appeared soon after eating sailfish fillets and included rashes, urticaria, nausea, vomiting, diarrhea, flushing, tingling and itching of the skin. The victims recovered within 8 h fish from victim tryptamine 208 ± 6 mg/100 g frozen fish fillet, Fried fish fillet-185 ± 11 mg/100 g; histamine 168 ± 8 and 180 ± 9 (normal appearance). Content of biogenic amines including tryptamine in fresh fish and fishery products, and emerging control strategies are discussed in the recent review by Arulkumar et al. [158].

Fresh broiler chicken cuts did not contain tryptamine in study conducted in Finland, 2004 [159]. Tryptamine was detected at last day of storage (12 d) (5.3–19 mg/kg). Phenylethylamine was detected in all samples at the beginning of storage. The level of concentration (9.0–22 mg/kg) did not change during the storage [159]. The formation of tyramine began immediately after packaging and at end of storage the tyramine concentration was over 200 mg/kg [159].

Attempts were undertaken to reduce the dose-dependent toxicity of biogenic amines [1]. Different approaches were used to manipulate the production of biogenic amines during manufacture and storage of food products [1].

Many plants, including strawflower and mistletoe, contain antioxidants and antimicrobials, which can increase the shelf life of seafood. Throughout history, mistletoe species were used as medicinal herbs. Phenolics compounds (e.g., flavonoids and chalcones, phthalides, a-pyron derivatives and terpenoids), essential oils, volatiles and fatty acids have been found in strawflowers. Strawflower suppressed biogenic amine accumulation in fish fillets [160]. The application of strawflower or mistletoe extract on trout fillets suppressed tyramine accumulation in fish meat ($p < 0.05$), although the fish treated with mistletoe extract had the highest level of tyramine at 20 days [160].

The effect of a multiple strain starter (KSL: *Kocuria varians*, *Staphylococcus xylosus* and *Lactobacillus sakei*) on the quality of soppressata molisana, a typical fermented dry-cured sausage produced in Southern Italy was investigated during 50 days of ripening [161]. Tryptamine level (mg/kg) reduced from 25.38 (standard deviation (SD) 1.85) in control batches manufactured without starter culture to 1.10 (SD 0.28) with KSL starter during 50 days of ripening [161]. During the same ripening period levels of total biogenic amines reduced from 130.6 ± 6.93 to 97.99 ± 2.83 (KSL) and 27.46 ± 3.44 (KSL+KCl). KSL with KCl, is experimental batch produced as KSL, except that 50 % (w/w) of NaCl was replaced with KCl in the mixture preparation.

Glucono-delta-lactone (GDL) was used at 1% to decrease pH in fresh minced meat samples incubated for 1, 3, and 7 days. The rate and level of pH decrease clearly affected biogenic amine formation in meat, indicating that the levels of histamine (up to 126 mg/ml) and tryptamine (up to 77 mg/kg) produced in meat could be decreased by optimizing the pH decrease during fermentation [162]. Addition of GDL decreased the levels of fecal streptococci, total aerobic bacteria, and coliforms.

Results showed a considerable antioxidant and anti-proliferative activity of garlic-supplemented Doenjang, a traditional Korean fermented soybean paste [163]. After 2 months of fermentation, the 1% heat-dried garlic and 3% freeze-dried garlic decrease (∼2-fold) the tryptamine level (4.58 mg/100 g) in control Doenjang containing no garlic.
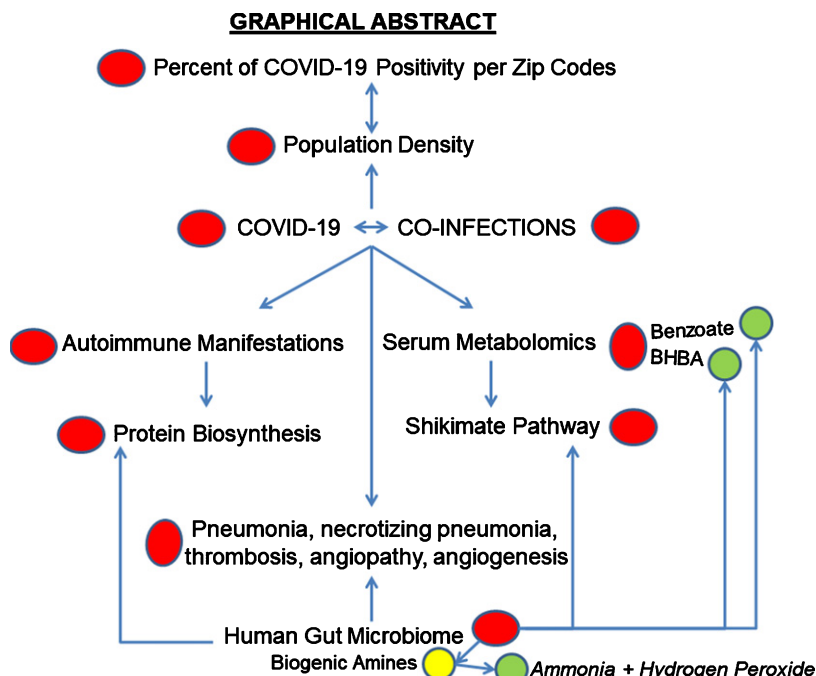
GRAPHICAL ABSTRACT

Percent of COVID-19 Positivity per Zip Codes

Population Density

COVID-19 ↔ CO-INFECTIONS

Autoimmune Manifestations   Serum Metabolomics   Benzoate BHBA

Protein Biosynthesis   Shikimate Pathway

Pneumonia, necrotizing pneumonia, thrombosis, angiopathy, angiogenesis

Human Gut Microbiome
Biogenic Amines   *Ammonia + Hydrogen Peroxide*

Fig. 1.

Hyperammonemia

Ammonia increase found in blood of both COVID-19 [19] and AD patients [20]. The liver plays a major role in regulating ammonia levels in the blood. Therefore, in liver disease the loss of hepatic function leads to hyperammonemia and increased brain ammonia and consequently hepatic encephalopathy (HE) [164]. Ammonia-lowering strategies remain the mainstay therapeutic strategy. Ammonia, both as an ion (NH4+) and gas (NH3), easily crosses all plasma membranes, including the BBB; the interface between the blood and the brain [164]. Glutamine synthetase (EC 6.3.1.2) found in bacteria catalyzes the condensation of glutamate and ammonium to form glutamine at the expense of ATP. L-glutamine is used in the shikimate pathway producing tryptophan in microorganisms. The data suggest that NH_3 enhances the transfer of tryptophan across the BBB [165]. In our study, tryptophan-dependent tRNA^{trp} aminoacylation catalyzed by TrpRS can be inhibited by its substrate tryptophan at physiological concentrations [3].

CONCLUSIONS

In this report, the author discusses the important subjects for understanding COVID-19: percentage of COVID-19 positivity by zip code's population in Florida, COVID-19 related autopsy cases from different countries, co-infections in COVID-19, serum metabolomics and autoantigenome of COVID-19, necrotizing pneumonia, and possible etiology of necrotizing conditions and intoxication in COVID-19 and other diseases, metabolites of microbial shikimate pathway in COVID-19 and other medical conditions and more (Fig. 1). Serum benzoate is more than 6-fold higher in COVID-19 and non-COVID-19 Chinese hospitalized patients compared to healthy control whereas benzoate is potentially toxic inhibitor of MAO. Sources of benzoate including food and disinfectants as well as benzoate biosynthesis and biodegradation are discussed in more details in different chapters of the book by Paley [2]. The data analysis presented here supports the inhibition of blood serum cholinesterases in patients with similar clinical characteristics including fever and/or cough.

I conclude here that necrotizing pneumonia was a risk factor for death in COVID-19 patients with hospital-acquired infection or co-infection with bacteria or other microorganisms that produce cytotoxic biogenic amines including tryptamine, which induce necrosis especially in the presence of a higher level of MAO inhibitor such as benzoate, and cholinesterase inhibitors including tryptamine. COVID-19 characterized with activation of microbial metabolic

shikimate pathway and of autoantigens' presentation especially enzymes of protein biosynthesis machinery. This can interfere with protein biosynthesis. The data on preexisting diseases and medical conditions associated with COVID-19 positivity indicate that those dying with—but not of—COVID-19 may still be infectious.

Of note, in the metabolomics study conducted at the Mayo Clinic, the blood plasma 2,4-dinitrophenol (DNP) is 2.017-fold higher ($p = 0.033$) and the CSF phenol is higher 1.48-fold ($p = 0.001$) in AD compared to controls [121]. Bacteria can produce benzoate from phenol [166]. Catechol occurs as an intermediate in the metabolism of both benzoate and phenol by strains of *Pseudomonas putida* [167]. DNP is a weight loss agent with significant acute toxicity and risk of death [168]. Ammonia and DNP are included in DHS (Department of Homeland Security) Chemicals of Interest (https://www.cisa.gov/sites/default/files/publications/appendix-a-to-part-27-508.pdf; Ammonia Security Issue is: Release 20,000 pounds minimum 20% – Toxic. DNP security issues are: Release - Screening Threshold Quantities in Pounds: 5,000; Theft in Pounds: 400.)

CONFLICT OF INTEREST

The authors have no conflict of interest to report'.

REFERENCES

[1]   Paley EL (2020) *Protein biosynthesis interference in disease*. Academic Press Book, Elsevier, pp. 1-296.
[2]   Paley EL (2021) *Microbial Metabolism and Disease*. Elsevier Science/Academic Press Book.
[3]   Paley EL, Denisova G, Sokolova O, Posternak N, Wang X, Brownell AL (2007) Tryptamine induces tryptophanyl-tRNA synthetase-mediated neurodegeneration with neurofibrillary tangles in human cell and mouse models. *Neuromolecular Med* **9**, 55-82.
[4]   Paley EL (2011) Tryptamine-induced tryptophanyl-tRNAtrp deficiency in neurodifferentiation and neurodegeneration interplay: Progenitor activation with neurite growth terminated in Alzheimer's disease neuronal vesicularization and fragmentation. *J Alzheimers Dis* **26**, 263-298.
[5]   Perry G (2020) Alzheimer's disease patients in the crosshairs of COVID-19. *J Alzheimers Dis* **76**, 1.
[6]   Paley EL, Merkulova-Rainon T, Faynboym A, Shestopalov VI, Aksenoff I (2018) Geographical distribution and diversity of gut microbial NADH:Ubiquinone oxidoreductase sequence associated with Alzheimer's disease. *J Alzheimers Dis* **61**, 1531-1540.
[7]   Paley EL (2019) Diet-related metabolic perturbations of gut microbial shikimate pathway-tryptamine-tRNA aminoacylation-protein synthesis in human health and disease. *Int J Tryptophan Res* **12**, 1178646919834550.
[8]   Paley EL (2019) Discovery of gut bacteria specific to Alzheimer's associated diseases is a clue to understanding disease etiology: Meta-analysis of population-based data on human gut metagenomics and metabolomics. *J Alzheimers Dis* **72**, 319-355.
[9]   Paley EL, Smelyanski L, Malinovskii V, Subbarayan PR, Berdichevsky Y, Posternak N, Gershoni JM, Sokolova O, Denisova G (2007) Mapping and molecular characterization of novel monoclonal antibodies to conformational epitopes on NH2 and COOH termini of mammalian tryptophanyl-tRNA synthetase reveal link of the epitopes to aggregation and Alzheimer's disease. *Mol Immunol* **44**, 541-557.
[10] Paley EL, Alexandrova N, Smelansky L (1995) Tryptophanyl-tRNA synthetase as a human autoantigen. *Immunol Lett* **48**, 201-207.
[11] Paley EL, Baranov VN, Alexandrova NM, Kisselev LL (1991) Tryptophanyl-tRNA synthetase in cell lines resistant to tryptophan analogs. *Exp Cell Res* **195**, 66-78.
[12] Paley EL (1999) Tryptamine-mediated stabilization of tryptophanyl-tRNA synthetase in human cervical carcinoma cell line. *Cancer Lett* **137**, 1-7.
[13] Rubin BY, Anderson SL, Xing L, Powell RJ, Tate WP (1991) Interferon induces tryptophanyl-tRNA synthetase expression in human fibroblasts. *J Biol Chem* **266**, 24245-24248.
[14] Shen T, Anderson SL, Rubin BY (1996) Use of alternative polyadenylation sites in the synthesis of mRNAs encoding the interferon-induced tryptophanyl tRNA synthetase. *Gene* **179**, 225-229.
[15] Goswami A, Wendt FR, Pathak GA, Tylee DS, De Angelis F, De Lillo A, Polimanti R (2021) Role of microbes in the pathogenesis of neuropsychiatric disorders. *Front Neuroendocrinol* **62**, 100917.
[16] Del Rio B, Redruello B, Fernandez M, Cruz Martin M, Ladero V, Alvarez MA (2020) The biogenic amine tryptamine, unlike β-phenylethyamine, shows *in vitro* cytotoxicity at concentrations that have been found in foods. *Food Chem* **331**, 127303.
[17] Luqman A, Nega M, Nguyen MT, Ebner P, Gotz F (2018) SadA-expressing Staphylococci in the human gut show increased cell adherence and internalization. *Cell Rep* **22**, 535-545.
[18] Luqman A, Ebner P, Reichert S, Sass P, Kabagema-Bilan C, Heilmann C, Ruth P, Gotz F (2019) A new host cell internalisation pathway for SadA-expressing staphylococci triggered by excreted neurochemicals. *Cell Microbiol* **21**, e13044.
[19] Bobermin LD, Quincozes-Santos A (2021) COVID-19 and hyperammonemia: Potential interplay between liver and brain dysfunctions. *Brain Behav Immun Health* **14**, 100257.
[20] Fisman M, Gordon B, Feleki V, Helmes E, Appell J, Rabheru K (1985) Hyperammonemia in Alzheimer's disease. *Am J Psychiatry* **142**, 71-73.
[21] Bortolato M, Chen K, Shih JC (2008) Monoamine oxidase inactivation: From pathophysiology to therapeutics. *Adv Drug Deliv Rev* **60**, 1527-1533.
[22] Vince AJ, Burridge SM (1980) Ammonia production by intestinal bacteria: The effects of lactose, lactulose and glucose. *J Med Microbiol* **13**, 177-191.
[23] Shen B, Yi X, Sun Y, Bi X, Du J, Zhang C, Quan S, Zhang F, Sun R, Qian L, Ge W, Liu W, Liang S, Chen H, Zhang Y, Li J, Xu J, He Z, Chen B, Wang J, Yan H, Zheng Y, Wang D,

Zhu J, Kong Z, Kang Z, Liang X, Ding X, Ruan G, Xiang N, Cai X, Gao H, Li L, Li S, Xiao Q, Lu T, Zhu Y, Liu H, Chen H, Guo T (2020) Proteomic and metabolomic characterization of COVID-19 patient sera. *Cell* **182**, 59-72 e15.

[24] Ala-Kokko TI, Tieranta N, Laurila J, Syrjala H (2001) Determinants of ICU mortality in necrotizing pancreatitis: The influence of Staphylococcus epidermidis. *Acta Anaesthesiol Scand* **45**, 853-857.

[25] Peng FCC (2016) Is Alzheimer's disease a fiction? *Clin Res Trials* **1**, doi: 10.15761/CRT.1000125

[26] Sathish T, Kapoor N, Cao Y, Tapp RJ, Zimmet P (2021) Proportion of newly diagnosed diabetes in COVID-19 patients: A systematic review and meta-analysis. *Diabetes Obes Metab* **23**, 870-874.

[27] Yourish K LK, Ivory D, Smith M (2020) Coronavirus deaths are nursing home residents or workers. *New York Times, May 09, 2020* https://wwwnytimescom/interactive/2020/05/09/us/coronavirus-cases-nursing-homes-ushtml.

[28] Wang M, Wei H, Zhao Y, Shang L, Di L, Lyu C, Liu J (2019) Analysis of multidrug-resistant bacteria in 3223 patients with hospital-acquired infections (HAI) from a tertiary general hospital in China. *Bosn J Basic Med Sci* **19**, 86-93.

[29] Tsalik EL, Li Y, Hudson LL, Chu VH, Himmel T, Limkakeng AT, Katz JN, Glickman SW, McClain MT, Welty-Wolf KE, Fowler VG, Ginsburg GS, Woods CW, Reed SD (2016) Potential cost-effectiveness of early identification of hospital-acquired infection in critically ill patients. *Ann Am Thorac Soc* **13**, 401-413.

[30] James BD, Leurgans SE, Hebert LE, Scherr PA, Yaffe K, Bennett DA (2014) Contribution of Alzheimer disease to mortality in the United States. *Neurology* **82**, 1045-1050.

[31] Bojanova DP, Bordenstein SR (2016) Fecal transplants: What is being transferred? *PLoS Biol* **14**, e1002503.

[32] Kim KO, Gluck M (2019) Fecal microbiota transplantation: An update on clinical practice. *Clin Endosc* **52**, 137-143.

[33] Eiseman B, Silen W, Bascom GS, Kauvar AJ (1958) Fecal enema as an adjunct in the treatment of pseudomembranous enterocolitis. *Surgery* **44**, 854-859.

[34] Chin SM, Sauk J, Mahabamunuge J, Kaplan JL, Hohmann EL, Khalili H (2017) Fecal microbiota transplantation for recurrent Clostridium difficile infection in patients with inflammatory bowel disease: A single-center experience. *Clin Gastroenterol Hepatol* **15**, 597-599.

[35] Dailey FE, Turse EP, Daglilar E, Tahan V (2019) The dirty aspects of fecal microbiota transplantation: A review of its adverse effects and complications. *Curr Opin Pharmacol* **49**, 29-33.

[36] Goloshchapov OV, Olekhnovich EI, Sidorenko SV, Moiseev IS, Kucher MA, Fedorov DE, Pavlenko AV, Manolov AI, Gostev VV, Veselovsky VA, Klimina KM, Kostryukova ES, Bakin EA, Shvetcov AN, Gumbatova ED, Klementeva RV, Shcherbakov AA, Gorchakova MV, Egozcue JJ, Pawlowsky-Glahn V, Suvorova MA, Chukhlovin AB, Govorun VM, Ilina EN, Afanasyev BV (2019) Long-term impact of fecal transplantation in healthy volunteers. *BMC Microbiol* **19**, 312.

[37] Brandt LJ (2012) Fecal transplantation for the treatment of Clostridium difficile infection. *Gastroenterol Hepatol (N Y)* **8**, 191-194.

[38] Ma Y, Chen H (2019) Faecal microbiota transplantation, a promising way to treat colorectal cancer. *EBioMedicine* **49**, 13-14.

[39] Li L, Li X, Zhong W, Yang M, Xu M, Sun Y, Ma J, Liu T, Song X, Dong W, Liu X, Chen Y, Liu Y, Abla Z, Liu W, Wang B, Jiang K, Cao H (2019) Gut microbiota from colorectal cancer patients enhances the progression of intestinal adenoma in Apc(min/+) mice. *EBioMedicine* **48**, 301-315.

[40] Wong SH, Zhao L, Zhang X, Nakatsu G, Han J, Xu W, Xiao X, Kwong TNY, Tsoi H, Wu WKK, Zeng B, Chan FKL, Sung JJY, Wei H, Yu J (2017) Gavage of fecal samples from patients with colorectal cancer promotes intestinal carcinogenesis in germ-free and conventional mice. *Gastroenterology* **153**, 1621-1633 e1626.

[41] Parasa S, Desai M, Thoguluva Chandrasekar V, Patel HK, Kennedy KF, Roesch T, Spadaccini M, Colombo M, Gabbiadini R, Artifon ELA, Repici A, Sharma P (2020) Prevalence of gastrointestinal symptoms and fecal viral shedding in patients with coronavirus disease 2019: A systematic review and meta-analysis. *JAMA Netw Open* **3**, e2011335.

[42] Wang X, Zheng J, Guo L, Yao H, Wang L, Xia X, Zhang W (2020) Fecal viral shedding in COVID-19 patients: Clinical significance, viral load dynamics and survival analysis. *Virus Res* **289**, 198147.

[43] Chang S, Pierson E, Koh PW, Gerardin J, Redbird B, Grusky D, Leskovec J (2021) Mobility network models of COVID-19 explain inequities and inform reopening. *Nature* **589**, 82-87.

[44] Rahmani AR, Leili M, Azarian G, Poormohammadi A (2020) Sampling and detection of corona viruses in air: A mini review. *Sci Total Environ* **740**, 140207.

[45] Zhu X, Ge Y, Wu T, Zhao K, Chen Y, Wu B, Zhu F, Zhu B, Cui L (2020) Co-infection with respiratory pathogens among COVID-2019 cases. *Virus Res* **285**, 198005.

[46] Lacy JM, Brooks EG, Akers J, Armstrong D, Decker L, Gonzalez A, Humphrey W, Mayer R, Miller M, Perez C, Arango JAR, Sathyavagiswaran L, Stroh W, Utley S (2020) COVID-19: Postmortem diagnostic and biosafety considerations. *Am J Forensic Med Pathol* **41**, 143-151.

[47] Bauer TT, Ewig S, Rodloff AC, Muller EE (2006) Acute respiratory distress syndrome and pneumonia: A comprehensive review of clinical data. *Clin Infect Dis* **43**, 748-756.

[48] Sato E, Yamamoto H, Honda T, Koyama S, Kubo K, Sediguchi M (1996) Acute respiratory distress syndrome due to methicillin-resistant Staphylococcus aureus sepsis in hyper-IgE syndrome. *Eur Respir J* **9**, 386-388.

[49] Goursaud S, Mombrun M, du Cheyron D (2020) COVID-19 necrotising pneumonia and extracorporeal membrane oxygenation: A challenge for anticoagulation. *ERJ Open Res* **6**, 00182-2020.

[50] Morris DE, Cleary DW, Clarke SC (2017) Secondary bacterial infections associated with influenza pandemics. *Front Microbiol* **8**, 1041.

[51] Farmen K, Tofiño-Vian M, Iovino F (2021) Neuronal damage and neuroinflammation, a bridge between bacterial meningitis and neurodegenerative diseases. *Front Cell Neurosci* **15**, doi: 10.3389/fncel.2021.680858

[52] Gezginc Y, Akyol I, Kuley E, Ozogul F (2013) Biogenic amines formation in Streptococcus thermophilus isolated from home-made natural yogurt. *Food Chem* **138**, 655-662.

[53] Özogul F, Özogul Y (2007) The ability of biogenic amines and ammonia production by single bacterial cultures. *Eur Food Res Technol* **225**, 385-394.

[54] Li L, Ruan L, Ji A, Wen Z, Chen S, Wang L, Wei X (2018) Biogenic amines analysis and microbial contribution

in traditional fermented food of Douchi. *Sci Rep* **8**, 12567.

[55]   Um I-S, Kim T, Kim H, Park K (2016) Characterization of tryptamine-producing bacteria isolated from commercial salted and fermented sand lance Ammodytes personatus sauces. *Korean J Fish Aquatic Sci* **49**, 792-799.

[56]   Diao M, Zhang S, Chen D, Hu W (2020) The novel coronavirus (COVID-19) infection in Hangzhou: An experience to share. *Cambridge University Press* **41**, 874-875.

[57]   McDanel JS, Perencevich EN, Storm J, Diekema DJ, Herwaldt L, Johnson JK, Winokur PL, Schweizer ML (2016) Increased mortality rates associated with Staphylococcus aureus and influenza co-infection, Maryland and Iowa, USA. *Emerg Infect Dis* **22**, 1253-1256.

[58]   Jia L, Zhao J, Yang C, Liang Y, Long P, Liu X, Qiu S, Wang L, Xie J, Li H, Liu H, Guo W, Wang S, Li P, Zhu B, Hao R, Ma H, Jiang Y, Song H (2018) Severe pneumonia caused by coinfection with influenza virus followed by methicillin-resistant Staphylococcus aureus induces higher mortality in mice. *Front Immunol* **9**, 3189.

[59]   Koehler P, Cornely OA, Bottiger BW, Dusse F, Eichenauer DA, Fuchs F, Hallek M, Jung N, Klein F, Persigehl T, Rybniker J, Kochanek M, Boll B, Shimabukuro-Vornhagen A (2020) COVID-19 associated pulmonary aspergillosis. *Mycoses* **63**, 528-534.

[60]   Meijer EFJ, Dofferhoff ASM, Hoiting O, Buil JB, Meis JF (2020) Azole-resistant COVID-19-associated pulmonary Aspergillosis in an immunocompetent host: A case report. *J Fungi (Basel)* **6**, 79.

[61]   Boaventura MAD, Lopes RFAP, Takahashi JA (2004) Microorganisms as tools in modern chemistry: The biotransformation of 3-indolylacetonitrile and tryptamine by fungi. *Braz J Microbiol* **35**, 345-347.

[62]   Sharifipour E, Shams S, Esmkhani M, Khodadadi J, Fotouhi-Ardakani R, Koohpaei A, Doosti Z, Ej Golzari S (2020) Evaluation of bacterial co-infections of the respiratory tract in COVID-19 patients admitted to ICU. *BMC Infect Dis* **20**, 646.

[63]   Grissinger M (2017) "Wrong patient" insulin pen injections alarmingly frequent even with barcode scanning. *P T* **42**, 550-552.

[64]   Brundage JF, Shanks GD (2008) Deaths from bacterial pneumonia during 1918-19 influenza pandemic. *Emerg Infect Dis* **14**, 1193-1199.

[65]   Morens DM, Taubenberger JK, Fauci AS (2008) Predominant role of bacterial pneumonia as a cause of death in pandemic influenza: Implications for pandemic influenza preparedness. *J Infect Dis* **198**, 962-970.

[66]   Wunderink RG, Waterer GW (2014) Community-acquired pneumonia. *N Engl J Med* **370**, 1863.

[67]   Gulick RM, Sobieszczyk ME, Landry DW, Hollenberg AN (2020) Prioritizing clinical research studies during the COVID-19 pandemic: Lessons from New York City. *J Clin Invest* **130**, 4522-4524.

[68]   Cummings MJ, Baldwin MR, Abrams D, Jacobson SD, Meyer BJ, Balough EM, Aaron JG, Claassen J, Rabbani LE, Hastie J, Hochman BR, Salazar-Schicchi J, Yip NH, Brodie D, O'Donnell MR (2020) Epidemiology, clinical course, and outcomes of critically ill adults with COVID-19 in New York City: A prospective cohort study. *Lancet* **395**, 1763-1770.

[69]   Goyal P, Choi JJ, Pinheiro LC, Schenck EJ, Chen R, Jabri A, Satlin MJ, Campion TR, Jr., Nahid M, Ringel JB, Hoffman KL, Alshak MN, Li HA, Wehmeyer GT, Rajan M, Reshetnyak E, Hupert N, Horn EM, Martinez FJ, Gulick

[70]   Liao KM, Ho CH, Ko SC, Li CY (2015) Increased risk of dementia in patients with chronic obstructive pulmonary disease. *Medicine (Baltimore)* **94**, e930.

[71]   Chen MH, Li CT, Tsai CF, Lin WC, Chang WH, Chen TJ, Pan TL, Su TP, Bai YM (2014) Risk of dementia among patients with asthma: A nationwide longitudinal study. *J Am Med Dir Assoc* **15**, 763-767.

[72]   Unruh MA, Yun H, Zhang Y, Braun RT, Jung HY (2020) Nursing home characteristics associated with COVID-19 deaths in Connecticut, New Jersey, and New York. *J Am Med Dir Assoc* **21**, 1001-1003.

[73]   Sen-Crowe B, Sutherland M, McKenney M, Elkbuli A (2020) The Florida COVID-19 mystery: Lessons to be learned. *Am J Emerg Med*, doi: 10.1016/j.ajem.2020. 08.009

[74]   Pomara C, Li Volti G, Cappello F (2020) COVID-19 deaths: Are we sure it is pneumonia? Please, autopsy, autopsy, autopsy! *J Clin Med* **9**, 1259.

[75]   Salerno M, Sessa F, Piscopo A, Montana A, Torrisi M, Patane F, Murabito P, Volti GL, Pomara C (2020) No autopsies on COVID-19 deaths: A missed opportunity and the lockdown of science. *J Clin Med* **9**, 1472.

[76]   Sperhake JP (2020) Autopsies of COVID-19 deceased? Absolutely! *Leg Med (Tokyo)* **47**, 101769.

[77]   Barton LM, Duval EJ, Stroberg E, Ghosh S, Mukhopadhyay S (2020) COVID-19 autopsies, Oklahoma, USA. *Am J Clin Pathol* **153**, 725-733.

[78]   Schaller T, Hirschbuhl K, Burkhardt K, Braun G, Trepel M, Markl B, Claus R (2020) Postmortem examination of patients with COVID-19. *JAMA* **323**, 2518-2520.

[79]   Carsana L, Sonzogni A, Nasr A, Rossi RS, Pellegrinelli A, Zerbi P, Rech R, Colombo R, Antinori S, Corbellino M, Galli M, Catena E, Tosoni A, Gianatti A, Nebuloni M (2020) Pulmonary post-mortem findings in a series of COVID-19 cases from northern Italy: A two-centre descriptive study. *Lancet Infect Dis* **20**, 1135-1140.

[80]   Lawrence MJ, Davies G, Nyberg M, Whitley J, Evans V, Williams R, Hellsten Y, Evans PA (2018) The effect of tyramine infusion and exercise on blood flow, coagulation and clot microstructure in healthy individuals. *Thromb Res* **170**, 32-37.

[81]   Chen N, Zhou M, Dong X, Qu J, Gong F, Han Y, Qiu Y, Wang J, Liu Y, Wei Y, Xia J, Yu T, Zhang X, Zhang L (2020) Epidemiological and clinical characteristics of 99 cases of 2019 novel coronavirus pneumonia in Wuhan, China: A descriptive study. *Lancet* **395**, 507-513.

[82]   Tang N, Li D, Wang X, Sun Z (2020) Abnormal coagulation parameters are associated with poor prognosis in patients with novel coronavirus pneumonia. *J Thromb Haemost* **18**, 844-847.

[83]   Mao L, Jin H, Wang M, Hu Y, Chen S, He Q, Chang J, Hong C, Zhou Y, Wang D, Miao X, Li Y, Hu B (2020) Neurologic manifestations of hospitalized patients with coronavirus disease 2019 in Wuhan, China. *JAMA Neurol* **77**, 683-690.

[84]   Beyrouti R, Adams ME, Benjamin L, Cohen H, Farmer SF, Goh YY, Humphries F, Jager HR, Losseff NA, Perry RJ, Shah S, Simister RJ, Turner D, Chandratheva A, Werring DJ (2020) Characteristics of ischaemic stroke associated with COVID-19. *J Neurol Neurosurg Psychiatry* **91**, 889-891.

[85]   Fox SE, Akmatbekov A, Harbert JL, Li G, Quincy Brown J, Vander Heide RS (2020) Pulmonary and cardiac

pathology in African American patients with COVID-19: An autopsy series from New Orleans. *Lancet Respir Med* **8**, 681-686.

[86] Solomon IH, Normandin E, Bhattacharyya S, Mukerji SS, Keller K, Ali AS, Adams G, Hornick JL, Padera RF, Jr., Sabeti P (2020) Neuropathological features of Covid-19. *N Engl J Med* **383**, 989-992.

[87] Menter T, Haslbauer JD, Nienhold R, Savic S, Hopfer H, Deigendesch N, Frank S, Turek D, Willi N, Pargger H, Bassetti S, Leuppi JD, Cathomas G, Tolnay M, Mertz KD, Tzankov A (2020) Postmortem examination of COVID-19 patients reveals diffuse alveolar damage with severe capillary congestion and variegated findings in lungs and other organs suggesting vascular dysfunction. *Histopathology* **77**, 198-209.

[88] Ackermann M, Verleden SE, Kuehnel M, Haverich A, Welte T, Laenger F, Vanstapel A, Werlein C, Stark H, Tzankov A, Li WW, Li VW, Mentzer SJ, Jonigk D (2020) Pulmonary vascular endothelialitis, thrombosis, and angiogenesis in Covid-19. *N Engl J Med* **383**, 120-128.

[89] Archer SL, Sharp WW, Weir EK (2020) Differentiating COVID-19 pneumonia from acute respiratory distress syndrome and high altitude pulmonary edema: Therapeutic implications. *Circulation* **142**, 101-104.

[90] Fried JA, Ramasubbu K, Bhatt R, Topkara VK, Clerkin KJ, Horn E, Rabbani L, Brodie D, Jain SS, Kirtane AJ, Masoumi A, Takeda K, Kumaraiah D, Burkhoff D, Leon M, Schwartz A, Uriel N, Sayer G (2020) The variety of cardiovascular presentations of COVID-19. *Circulation* **141**, 1930-1936.

[91] Paley EL, Perry G (2018) Towards an integrative understanding of tRNA aminoacylation-diet-host-gut microbiome interactions in neurodegeneration. *Nutrients* **10**, 410.

[92] Cacciatore F, Gaudiosi C, Mazzella F, Scognamiglio A, Mattucci I, Carone M, Ferrara N, Abete P (2017) Pneumonia and hospitalizations in the elderly. *Geriatric Care* **3**, 20-28.

[93] Jackson ML, Neuzil KM, Thompson WW, Shay DK, Yu O, Hanson CA, Jackson LA (2004) The burden of community-acquired pneumonia in seniors: Results of a population-based study. *Clin Infect Dis* **39**, 1642-1650.

[94] Erichsen Andersson A, Egerod I, Knudsen VE, Fagerdahl AM (2018) Signs, symptoms and diagnosis of necrotizing fasciitis experienced by survivors and family: A qualitative Nordic multi-center study. *BMC Infect Dis* **18**, 429.

[95] Orii KO, Iwao Y, Higuchi W, Takano T, Yamamoto T (2010) Molecular characterization of methicillin-resistant Staphylococcus aureus from a fatal case of necrotizing fasciitis in an extremely low-birth-weight infant. *Clin Microbiol Infect* **16**, 289-292.

[96] Peker E, Kirimi E, Tuncer O, Ceylan A, Cagan E, Dogan M (2010) Necrotizing fasciitis caused by Staphylococcus epidermidis in a neonate with extremely low birthweight. *J Dermatol* **37**, 671-673.

[97] Perbet S, Soummer A, Vinsonneau C, Vandebrouck A, Rackelboom T, Etienne J, Cariou A, Chiche JD, Mira JP, Charpentier J (2010) Multifocal community-acquired necrotizing fasciitis caused by a Panton-Valentine leukocidin-producing methicillin-sensitive Staphylococcus aureus. *Infection* **38**, 223-225.

[98] Aswani V, Mau B, Shukla SK (2016) Complete genome sequence of Staphylococcus aureus MCRF184, a necrotizing fasciitis-causing methicillin-sensitive sequence type 45 staphylococcus strain. *Genome Announc* **4**, e00374-16.

[99] Kim W, Seo JM (2020) Necrotizing enterocolitis. *N Engl J Med* **383**, 2461.

[100] Kim JH, Sampath V, Canvasser J (2020) Challenges in diagnosing necrotizing enterocolitis. *Pediatr Res* **88**, 16-20.

[101] Liu RX, Johnson A (1984) Necrotizing enterocolitis with epidemic Staphylococcus in a neonatal intensive care unit. *Chin Med J (Engl)* **97**, 278-282.

[102] Lemyre B, Xiu W, Bouali NR, Brintnell J, Janigan JA, Suh KN, Barrowman N (2012) A decrease in the number of cases of necrotizing enterocolitis associated with the enhancement of infection prevention and control measures during a Staphylococcus aureus outbreak in a neonatal intensive care unit. *Infect Control Hosp Epidemiol* **33**, 29-33.

[103] Schmid SW, Uhl W, Friess H, Malfertheiner P, Buchler MW (1999) The role of infection in acute pancreatitis. *Gut* **45**, 311-316.

[104] Bracci PM, Wang F, Hassan MM, Gupta S, Li D, Holly EA (2009) Pancreatitis and pancreatic cancer in two large pooled case-control studies. *Cancer Causes Control* **20**, 1723-1731.

[105] Sadr-Azodi O, Oskarsson V, Discacciati A, Videhult P, Askling J, Ekbom A (2018) Pancreatic cancer following acute pancreatitis: A population-based matched cohort study. *Am J Gastroenterol* **113**, 1711-1719.

[106] Pirila L, Soderstrom KO, Hietarinta M, Jalava J, Kyto V, Toivanen A (2006) Fatal myocardial necrosis caused by Staphylococcus lugdunensis and cytomegalovirus in a patient with scleroderma. *J Clin Microbiol* **44**, 2295-2297.

[107] Heo S, Lee JH, Jeong DW (2020) Food-derived coagulase-negative Staphylococcus as starter cultures for fermented foods. *Food Sci Biotechnol* **29**, 1023-1035.

[108] Short KR, Diavatopoulos DA, Thornton R, Pedersen J, Strugnell RA, Wise AK, Reading PC, Wijburg OL (2011) Influenza virus induces bacterial and nonbacterial otitis media. *J Infect Dis* **204**, 1857-1865.

[109] Rowe HM, Meliopoulos VA, Iverson A, Bomme P, Schultz-Cherry S, Rosch JW (2019) Direct interactions with influenza promote bacterial adherence during respiratory infections. *Nat Microbiol* **4**, 1328-1336.

[110] Deeb SS, Moyle EA (1982) Stability of Lambdoid bacteriophage heads: Antagonism between polyamines and tryptamine. *J Virol* **43**, 753-755.

[111] Wang JY, Zhang W, Roehrl MW, Roehrl VB, Roehrl MH (2021) An autoantigen atlas from human lung HFL1 cells offers clues to neurological and diverse autoimmune manifestations of COVID-19. *bioRxiv*, 2021.2001.2024.427965.

[112] Jobin PG, Solis N, Machado Y, Bell PA, Kwon NH, Kim S, Overall CM, Butler GS (2019) Matrix metalloproteinases inactivate the proinflammatory functions of secreted moonlighting tryptophanyl-tRNA synthetase. *J Biol Chem* **294**, 12866-12879.

[113] Zhou Z, Sun B, Nie A, Yu D, Bian M (2020) Roles of aminoacyl-tRNA synthetases in cancer. *Front Cell Dev Biol* **8**, 599765.

[114] Filonenko VV, Beresten SF, Rubikaite BI, Kisselev LL (1989) Bovine tryptophanyl-tRNA synthetase and glyceraldehyde-3-phosphate dehydrogenase form a complex. *Biochem Biophys Res Commun* **161**, 481-488.

[115] Lee HC, Lee ES, Uddin MB, Kim TH, Kim JH, Chathuranga K, Chathuranga WAG, Jin M, Kim S, Kim CJ, Lee JS (2019) Released tryptophanyl-tRNA synthetase stimulates

innate immune responses against viral infection. *J Virol* **93**, e01291-18.

[116] Yeung ML, Jia L, Yip CCY, Chan JFW, Teng JLL, Chan KH, Cai JP, Zhang C, Zhang AJ, Wong WM, Kok KH, Lau SKP, Woo PCY, Lo JYC, Jin DY, Shih SR, Yuen KY (2018) Human tryptophanyl-tRNA synthetase is an IFN-gamma-inducible entry factor for Enterovirus. *J Clin Invest* **128**, 5163-5177.

[117] Wang JY, Zhang W, Roehrl MW, Roehrl VB, Roehrl MH (2021) An autoantigen-ome from HS-sultan B-Lymphoblasts offers a molecular map for investigating autoimmune sequelae of COVID-19. *bioRxiv*, https://doi.org/10.1101/2021.04.05.438500.

[118] Zarmouh NO, Messeha SS, Elshami FM, Soliman KF (2016) Evaluation of the Isoflavone Genistein as Reversible Human Monoamine Oxidase-A and -B Inhibitor. *Evid Based Complement Alternat Med* **2016**, 1423052.

[119] Bansal Y, Singh R, Parhar I, Kuhad A, Soga T (2019) Quinolinic acid and nuclear factor erythroid 2-related factor 2 in depression: Role in neuroprogression. *Front Pharmacol* **10**, 452.

[120] Egashira T, Sakai K, Takayama F, Sakurai M, Yoshida S (2003) Zinc benzoate, a contaminating environmental compound derived from polystyrene resin inhibits A-type monoamine oxidase. *Toxicol Lett* **145**, 161-165.

[121] Trushina E, Dutta T, Persson XM, Mielke MM, Petersen RC (2013) Identification of altered metabolic pathways in plasma and CSF in mild cognitive impairment and Alzheimer's disease using metabolomics. *PLoS One* **8**, e63644.

[122] Clinton CM, Bain JR, Muehlbauer MJ, Li Y, Li L, O'Neal SK, Hughes BL, Cantonwine DE, McElrath TF, Ferguson KK (2020) Non-targeted urinary metabolomics in pregnancy and associations with fetal growth restriction. *Sci Rep* **10**, 5307.

[123] Van Bever HP, Docx M, Stevens WJ (1989) Food and food additives in severe atopic dermatitis. *Allergy* **44**, 588-594.

[124] Lennerz BS, Vafai SB, Delaney NF, Clish CB, Deik AA, Pierce KA, Ludwig DS, Mootha VK (2015) Effects of sodium benzoate, a widely used food preservative, on glucose homeostasis and metabolic profiles in humans. *Mol Genet Metab* **114**, 73-79.

[125] Williams HR, Cox IJ, Walker DG, North BV, Patel VM, Marshall SE, Jewell DP, Ghosh S, Thomas HJ, Teare JP, Jakobovits S, Zeki S, Welsh KI, Taylor-Robinson SD, Orchard TR (2009) Characterization of inflammatory bowel disease with urinary metabolic profiling. *Am J Gastroenterol* **104**, 1435-1444.

[126] Williams HR, Cox IJ, Walker DG, Cobbold JF, Taylor-Robinson SD, Marshall SE, Orchard TR (2010) Differences in gut microbial metabolism are responsible for reduced hippurate synthesis in Crohn's disease. *BMC Gastroenterol* **10**, 108.

[127] Goedert JJ, Sampson JN, Moore SC, Xiao Q, Xiong X, Hayes RB, Ahn J, Shi J, Sinha R (2014) Fecal metabolomics: Assay performance and association with colorectal cancer. *Carcinogenesis* **35**, 2089-2096.

[128] Srinivasan S, Morgan MT, Fiedler TL, Djukovic D, Hoffman NG, Raftery D, Marrazzo JM, Fredricks DN (2015) Metabolic signatures of bacterial vaginosis. *MBio* **6**, e00204-15.

[129] Nelson TM, Borgogna JC, Michalek RD, Roberts DW, Rath JM, Glover ED, Ravel J, Shardell MD, Yeoman CJ, Brotman RM (2018) Cigarette smoking is associated with an altered vaginal tract metabolomic profile. *Sci Rep* **8**, 852.

[130] Husson MC, Schiff M, Fouilhoux A, Cano A, Dobbelaere D, Brassier A, Mention K, Arnoux JB, Feillet F, Chabrol B, Guffon N, Elie C, de Lonlay P (2016) Efficacy and safety of i.v. sodium benzoate in urea cycle disorders: A multicentre retrospective study. *Orphanet J Rare Dis* **11**, 127.

[131] Manaf FA, Lawler N, Peiffer JJ, Maker GL, Boyce MC, Fairchild TJ, Broadhurst D (2018) Characterizing the plasma metabolome during and following a maximal exercise cycling test. *J Appl Physiol (1985)* **125**, 1193-1203.

[132] Thomas T, Stefanoni D, Reisz JA, Nemkov T, Bertolone L, Francis RO, Hudson KE, Zimring JC, Hansen KC, Hod EA, Spitalnik SL, D'Alessandro A (2020) COVID-19 infection alters kynurenine and fatty acid metabolism, correlating with IL-6 levels and renal status. *JCI Insight* **5**, e140327.

[133] Lv L, Jiang H, Chen Y, Gu S, Xia J, Zhang H, Lu Y, Yan R, Li L (2021) The faecal metabolome in COVID-19 patients is altered and associated with clinical features and gut microbes. *Anal Chim Acta* **1152**, 338267.

[134] Wu L, Han Y, Zheng Z, Peng G, Liu P, Yue S, Zhu S, Chen J, Lv H, Shao L, Sheng Y, Wang Y, Li L, Li L, Wang B (2021) Altered gut microbial metabolites in amnestic mild cognitive impairment and Alzheimer's disease: Signals in host-microbe interplay. *Nutrients* **13**, 228.

[135] Won C, Shen X, Mashiguchi K, Zheng Z, Dai X, Cheng Y, Kasahara H, Kamiya Y, Chory J, Zhao Y (2011) Conversion of tryptophan to indole-3-acetic acid by tryptophan aminotransferases of arabidopsis and yuccas in Arabidopsis. *Proc Natl Acad Sci U S A* **108**, 18518-18523.

[136] Koshima H, Honke S (1999) Chiral bimolecular crystallization of tryptamine and achiral carboxylic acids. *J Org Chem* **64**, 790-793.

[137] Koshima H, Honke S, Fujita J (1999) Generation of chirality in two-component molecular crystals of tryptamine and achiral carboxylic acids. *J Org Chem* **64**, 3916-3921.

[138] Kaddurah-Daouk R, Zhu H, Sharma S, Bogdanov M, Rozen SG, Matson W, Oki NO, Motsinger-Reif AA, Churchill E, Lei Z, Appleby D, Kling MA, Trojanowski JQ, Doraiswamy PM, Arnold SE, Pharmacometabolomics Research Network (2013) Alterations in metabolic pathways and networks in Alzheimer's disease. *Transl Psychiatry* **3**, e244.

[139] Paley E (1999-2001) Tryptamine treated, human differentiated, neuronal Alzheimer-like cell and attendant methods of cell modeling. In *Google Patents*, USPTO, USA.

[140] Paley EL, Perry G, Sokolova O (2013) Tryptamine induces axonopathy and mitochondriopathy mimicking neurodegenerative diseases via tryptophanyl-tRNA deficiency. *Curr Alzheimer Res* **10**, 987-1004.

[141] Mendes R (2009) Biogenic amines. In *Fishery Products*, pp. 42-67.

[142] Wright CI, Guela C, Mesulam MM (1993) Protease inhibitors and indoleamines selectively inhibit cholinesterases in the histopathologic structures of Alzheimer disease. *Proc Natl Acad Sci U S A* **90**, 683-686.

[143] Nicolet Y, Lockridge O, Masson P, Fontecilla-Camps JC, Nachon F (2003) Crystal structure of human butyrylcholinesterase and of its complexes with substrate and products. *J Biol Chem* **278**, 41141-41147.

[144] Wan L, Lu J, Fu J, Huang J, Yang Q, Xin B, Chen L, Huo Y, Zhong Y, Guo C (2018) Acetylcholinesterase inhibitor donepezil effects on plasma beta-hydroxybutyrate levels

in the treatment of Alzheimer's disease. *Curr Alzheimer Res* **15**, 917-927.

[145] Sankaranarayanan K, Ozga AT, Warinner C, Tito RY, Obregon-Tito AJ, Xu J, Gaffney PM, Jervis LL, Cox D, Stephens L, Foster M, Tallbull G, Spicer P, Lewis CM (2015) Gut microbiome diversity among Cheyenne and Arapaho individuals from Western Oklahoma. *Curr Biol* **25**, 3161-3169.

[146] Newman JC, Verdin E (2014) beta-hydroxybutyrate: Much more than a metabolite. *Diabetes Res Clin Pract* **106**, 173-181.

[147] Wang CY, Wu CL, Tsan YT, Hsu JY, Hung DZ, Wang CH (2010) Early onset pneumonia in patients with cholinesterase inhibitor poisoning. *Respirology* **15**, 961-968.

[148] Depczynski B, Lee ATK, Varndell W, Chiew AL (2019) The significance of an increased beta-hydroxybutyrate at presentation to the emergency department in patients with diabetes in the absence of a hyperglycemic emergency. *J Diabetes Res* **2019**, 7387128.

[149] Kanikarla-Marie P, Jain SK (2016) Hyperketonemia and ketosis increase the risk of complications in type 1 diabetes. *Free Radic Biol Med* **95**, 268-277.

[150] Bailey SR, Marr CM, Elliott J (2003) Identification and quantification of amines in the equine caecum. *Res Vet Sci* **74**, 113-118.

[151] Takaki M, Mawe GM, Barasch JM, Gershon MD, Gershon MD (1985) Physiological responses of guinea-pig myenteric neurons secondary to the release of endogenous serotonin by tryptamine. *Neuroscience* **16**, 223-240.

[152] Takaki M, Mizutani M, Jin JG, Nakayama S (1990) Slow hyperpolarizing action of tryptamine on myenteric neurons of the isolated guinea-pig ileum. *Acta Med Okayama* **44**, 87-91.

[153] Schmitt M, Böhm M, Ratzer C, Vu C, Kalkman I, Meerts WL (2005) Structural selection by microsolvation: Conformational locking of tryptamine. *J Am Chem Soc* **127**, 10356-10364.

[154] Medina MA, Urdiales JL, Rodriguez-Caso C, Ramirez FJ, Sanchez-Jimenez F (2003) Biogenic amines and polyamines: Similar biochemistry for different physiological missions and biomedical applications. *Crit Rev Biochem Mol Biol* **38**, 23-59.

[155] Hellstrand K (2002) Histamine in cancer immunotherapy: A preclinical background. *Semin Oncol* **29**, 35-40.

[156] Hellstrand K, Hermodsson S, Brune M, Naredi P, Carneskog J, Mellqvist UH (1997) Histamine in cancer immunotherapy. *Scand J Clin Lab Invest* **57**, 193-202.

[157] Hwang D-F, Chang S-H, Shiau C-Y, Cheng C-C (1995) Biogenic amines in the flesh of sailfish (Istiophorus plafypferus) responsible for scornbroid poisoning. *J Food Sci* **60**, 926-928.

[158] Arulkumar A, Paramithiotis S, Paramasivam S (2001) Biogenic amines in fresh fish and fishery products and emerging control. *Aquac Fish*, doi: 10.1016/j.aaf.2021.02.001

[159] Rokka M, Eerola S, Smolander M, Alakomi H-L, Ahvenainen R (2004) Monitoring of the quality of modified atmosphere packaged broiler chicken cuts stored in different temperature conditions: B. Biogenic amines as quality-indicating metabolites. *Food Control* **15**, 601-607.

[160] Özogul F, Kus B, Kuley E (2013) The impact of strawflower and mistletoe extract on quality properties of rainbow trout fillets. *Int J Food Sci Technol* **48**, 2228-2238.

[161] Di Luccia A, Tremonte P, Trani A, Loizzo P, La Gatta B, Succi M, Sorrentino E, Coppola R (2016) Influence of starter cultures and KCl on some biochemical, microbiological and sensory features of soppressata molisana, an Italian fermented sausage. *Eur Food Res Technol* **242**, 855-867.

[162] Maijala RL, Eerola SH, Aho MA, Hirn JA (1993) The effect of GDL-induced pH decrease on the formation of biogenic amines in meat. *J Food Prot* **56**, 125-129.

[163] Bahuguna A, Shukla S, Lee JS, Bajpai VK, Kim SY, Huh YS, Han YK, Kim M (2019) Garlic augments the functional and nutritional behavior of Doenjang, a traditional Korean fermented soybean paste. *Sci Rep* **9**, 5436.

[164] Oliveira M, Tremblay, M, Rose, CF (2018) A195 Glutamine synthetase in endothelial cells of the blood-brain barrier: New target for the treatment of hepatic encephalopathy? *J Can Assoc Gastroenterol* **1**(Suppl 1), 340–341.

[165] Grippon P, Le Poncin Lafitte M, Boschat M, Wang S, Faure G, Dutertre D, Opolon P (1986) Evidence for the role of ammonia in the intracerebral transfer and metabolism of tryptophan. *Hepatology* **6**, 682-686.

[166] Juteau P, Cote V, Duckett MF, Beaudet R, Lepine F, Villemur R, Bisaillon JG (2005) Cryptanaerobacter phenolicus gen. nov., sp. nov., an anaerobe that transforms phenol into benzoate via 4-hydroxybenzoate. *Int J Syst Evol Microbiol* **55**, 245-250.

[167] Feist CF, Hegeman GD (1969) Phenol and benzoate metabolism by Pseudomonas putida: Regulation of tangential pathways. *J Bacteriol* **100**, 869-877.

[168] Grundlingh J, Dargan PI, El-Zanfaly M, Wood DM (2011) 2,4-dinitrophenol (DNP): A weight loss agent with significant acute toxicity and risk of death. *J Med Toxicol* **7**, 205-212.